NUREG/CR-3369
SAND83-1438
R1
Printed May 1984

An Uncertainty Study of PWR Steam Explosions

M. Berman, D. V. Swenson, A. J. Wickett

Prepared by
Sandia National Laboratories
Albuquerque, New Mexico 87185 and Livermore, California 94550
for the United States Department of Energy
under Contract DE-AC04-76DP00789

Prepared for
U. S. NUCLEAR REGULATORY COMMISSION

Available from

GPO Sales Program
Division of Technical Information and Document Control
U.S. Nuclear Regulatory Commission
Washington, D.C. 20555

and

National Technical Information Service
Springfield, Virginia 22161

NUREG/CR-3369
SAND83-1438
R1

AN UNCERTAINTY STUDY OF PWR STEAM EXPLOSIONS

M. Berman, D. V. Swenson* and A. J. Wickett+

MAY 1984

Sandia National Laboratories
Albuquerque, NM 87185
Operated by
Sandia Corporation
for the
U. S. Department of Energy

Prepared for
Division of Accident Evaluation
Office of Nuclear Regulatory Research
U. S. Nuclear Regulatory Commission
Washington, DC 20555
Under Memorandum of Understanding DOE 40-550-75
NRC FIN No. A1030

*Present address: School of Civil and Environmental Engineering, Cornell University, Hollister Hall, Ithaca, NY 14853

+On attachment from United Kingdom Atomic Energy Authority, Safety and Reliability Directorate

Abstract

Some previous assessments of the probability of containment failure caused by in-vessel steam explosions in a PWR have recognized large uncertainties and assigned broad ranges to the probability, while others have concluded that the probability is small or zero. In this report we study the uncertainty in the probability of containment failure by combining the uncertainties in the component physical processes using a Monte Carlo method. We conclude that, despite substantial research, the combined uncertainty is still large. Some areas are identified in which improvements in our understanding may lead to large reductions in the overall uncertainty.

CONTENTS

CONTENTS (cont'd)

Illustrations

Tables

List of Abbreviations

BWR	Boiling Water Reactor
CEA	Commissariat a l'Energie Atomique
EDF	Electricite de France
EPRI	Electric Power Research Institute
EXO-FITS	FITS experiments conducted outdoors
FITS	Fully Instrumented Test Series
LANL	Los Alamos National Laboratory
LWR	Light Water Reactor
NDRC	National Defense Research Committee
PWR	Pressurized Water Reactor
RPV	Reactor Pressure Vessel
UIS	Upper Internal Structure
UKAEA	United Kingdom Atomic Energy Authority
WASH-1400	Reactor Safety Study [Reference 1]
ZIP	Zion/Indian Point Study [References 2 and 3]

ACKNOWLEDGEMENT

Many individuals with diverse backgrounds contributed to this study. M. L. Corradini, R. G. Easterling, N. A. Evans, D. E. Mitchell and J. B. Rivard all attended meetings of a Working Group and participated in discussions with the authors dealing with the phenomenological and statistical questions that arise in this kind of study. Their contributions are gratefully acknowledged by the authors.

In addition to valuable assistance from reviewers within Sandia National Laboratories, we acknowledge helpful comments from R. S. Peckover (UKAEA), D. Squarer (EPRI), and J. L. Telford (NRC)

Summary

In the unlikely event of a core-melt accident in a PWR, molten core material may flow down into residual water in the lower plenum of the reactor pressure vessel, possibly resulting in a steam explosion. The probability that such an explosion would be large enough to fail containment, for example by ejecting the vessel top sufficiently energetically, is of interest for probabilistic risk assessment.

Many studies have addressed this issue [1, 4-12], and have offered a variety of probability estimates covering several orders of magnitude. One of these studies [11] investigated the probability by assigning probability distributions to various uncertain parameters in a simple model of the process, and then sampling at random in a Monte Carlo analysis. The number of containment failures predicted by the model, out of 10,000 trials, gave the probability of containment failure.

The present study has two major goals. The first is to provide an uncertainty estimate for the conditional probability of direct containment failure by steam explosions (given core melt). The second is to identify important contributors to this uncertainty, in order to provide understanding of the reasons for its magnitude and to indicate (by sensitivity studies) what additional information would be needed to reduce it.

This report offers several improvements over the previous analysis [11]. Uncertainties have been evaluated in a more complete and systematic manner. The input distributions have also been chosen more consistently, and the uncertainty ranges have been explored in greater depth by sampling portions of the ranges with separate distributions. Changes have been made in the modeling of the physical processes described. Among the most important of these were: changes in the calculation of the amount of melt that can participate in the explosion; changes in the conversion ratio estimates; changes in the calculation of the energy absorbed by the internal structure; and changes in modeling slug impact and vessel and containment failure. The distributions and uncertainty estimates also reflect some recent research results.

When distributions were selected from the lower thirds of the uncertainty ranges, the probability of failing both the PWR vessel lower plenum and the large, dry containment was zero. When distributions from the middle thirds of the uncertainty ranges were used, the probability of containment failure was essentially zero (i.e., approximately 10^{-4}). The corresponding probabilty of failing the lower plenum of the vessel was about 21%. When distributions from the high thirds of the uncertainty ranges were used, the probability of failing both the vessel and containment was very nearly one. The individual

probability numbers calculated would have been different had a different parameterization of the problem been used. However, the ranges of uncertainty calculated for these probabilities covers the entire range of possibilities.

Sensitivity studies indicated that among the most important uncertainties were those in the pour diameter (related to total mass of molten core mixed) and conversion ratio. When the distributions of each of these parameters were taken at the upper third of their ranges, all other parametric distributions remaining in the middle of their parameter ranges, the probabilities of vessel and containment failure increased significantly. Similarly, when these parameters were sampled in the lower third of their uncertainty ranges, the failure probabilities were significantly reduced, even when all other parameters were sampled at the high parts of their ranges.

The modeling described above refers to accidents in which the pressure in the reactor vessel is at or near atmospheric. Extensions of these results to accidents that occur at higher ambient pressures in the vessel introduces additional uncertainty. There may well be differences in mixing, triggering, conversion ratio and vessel failure due to higher ambient pressure, but the current state of knowledge is insufficient to account for these differences.

The calculations reported here assumed that strong enough loading of the reactor pressure vessel upper head would produce a large missile, rather than a more benign failure mode. A large missile, if energetic enough, could penetrate the containment; if the explosion produced only small missiles or none at all, the large dry containment would very likely remain intact. Thus the pressure vessel failure mode is another important uncertainty.

For consistency in these calculations, dimensions were taken from the Zion PWRs. The results calculated in this report may, in principle, be extended to other PWRs by accounting for differences in geometry, containment strength, missile shields, etc. Application to BWRs entails a large uncertainty because of major plant differences. Differences in BWR vessel geometry and strength could strongly affect the characteristics of the steam explosion. Differences in containment geometry and strength will also influence the failure mode (penetration by missiles or overpressurization due to rapid steam release).

1. Introduction

1.1 Background

Although accidents in light water reactors (LWRs) involving core melting, breach of containment, and release of radionuclides to the environment are unlikely events, they were considered in the Reactor Safety Study of 1975 [1] and have received renewed research emphasis since the accident at Three Mile Island Unit 2 in March of 1979.

The analysis of such accidents requires consideration of phenomena accompanying damage to the core which could cause a breach in containment allowing the release of radioactive materials outside the plant. Severe damage to the reactor core will occur because of overheating by decay heat, even if the reactor is shut down, if the core ceases to be covered with cooling water and remains uncovered for longer than about 10 to 30 minutes (depending on accident scenario). The core will be uncovered either if the primary circuit leaks and the lost coolant is not replenished (loss-of-coolant accident) or if the capability to remove decay heat from the primary circuit is lost, in which case the coolant will boil off through safety valves uncovering the core unless, again, coolant is replenished. Severe fuel damage will begin if the fuel temperature exceeds about 1300 K at which point rapid oxidation of the zircaloy cladding begins. If reflooding with water does not occur, the core will continue to be heated by decay heat and exothermic clad oxidation until melting begins at about 2000 K (the melting point of zircaloy). Gross fuel liquefaction may begin at this point (UO_2 is soluble in liquid zircaloy under some circumstances) or it may be postponed as late as the time at which the melting point of UO_2, about 3100 K, is reached. When gross liquefaction occurs the melt will at first flow down and refreeze on cooler fuel below. At this point a number of alternatives exist. One possibility is that an impermeable crust forms at the bottom of the core, holding up subsequently formed melt in a pool; another possibility is that such a crust does not form in which case the melt will flow out from the base of the core as it is formed. In the latter case the melt will be steadily quenched by residual water in the lower plenum of the reactor pressure vessel (RPV); the water will steadily boil off. Whether these or other processes occur is highly uncertain.

The former case leads to the possibility that when the melt pool becomes so large that the crust can no longer hold it up, it may coherently flow down into residual liquid water in the lower plenum of the reactor pressure vessel, possibly causing a steam explosion which might be large enough to eject a missile that could breach the containment building. Such a sequence of events would be of high significance to risk because it would breach two barriers to the release of radioactivity, the RPV and the containment building, almost simultaneously. If these barriers were

breached simultaneously there would be a path for release of radionuclides to the environment potentially affording little attenuation. These events may occur relatively soon (~ 1 hour) after reactor shutdown which also enhances the possibility that the release of radioactivity would be large.

A steam explosion is caused by the rapid transfer of thermal energy from a hot liquid (in this case liquefied core material) to water on a time scale so short (~ 1 ms) as to produce effects associated with the more familiar chemical explosives. Industrial experience with these thermal explosions [13] has shown them to be often capable of doing significant damage.

An important issue which emerges from these considerations is the need to estimate the probability that, given the required conditions (liquefied core materials contacting liquid coolant), a containment-breaching steam explosion will occur. This is the "conditional probability" discussed in this document.

A second issue which emerges is the need to assess the degree of certainty which may be attached to the probability estimate described above. One way to perform such an uncertainty assessment is to provide bounds which express the range within which we are confident the probability lies. If the bounds turn out to be suitably narrow or skewed to the low probability side, we may conclude that a probability estimate within these bounds is satisfactory and that further effort to refine the estimate is unnecessary. On the other hand, wide bounds that include the possibility of high conditional probabilities may signal the need for improved resolution of the issue.

This study addresses the steam explosion issue for a pressurized water reactor (PWR) located in a large dry containment structure (for convenience only, data were taken from the Zion PWRs [14]. The reader is cautioned not to apply the results given here to other reactor or containment types without appropriate reformulation of the problem.

1.2 Previous Assessments

The Reactor Safety Study [1] contains the first quantitative analysis of this problem. Its authors concluded that "a broad band of uncertainty must be associated with a quantitative evaluation of the likelihood of failure of the containment as a result of a steam explosion in the primary vessel." To express such consensus as they had achieved, they adopted a range 10^{-1} to 10^{-4} for the conditional probability of containment failure, given core melt. (These numbers were the fifth and 95th percentiles of a skew log-normal distribution whose median was 10^{-2}.) It was thus clear in 1975 that further investigation was necessary.

The German Risk Study [4] came to essentially the same conclusions in 1979; on the one hand "a destruction of the containment vessel as a result of a steam explosion is very unlikely," but on the other, problems of meltdown, fragmentation and heat transfer were "open", leaving a degree of uncertainty reflected in the range 10^{-1} to 10^{-3} chosen for the conditional probability of containment failure (fifth and 95th percentiles, lognormal distribution, median 10^{-2}), pending the results of further research.

The recent (1982) UKAEA PWR Degraded Core Analysis Report [5] took a similar view, stating "despite recent work the uncertainty properly recognized by the Reactor Safety Study and the German Risk Study has not been significantly diminished and we see no reason to adopt a narrower range than that of the Reactor Safety Study."

The view expressed by the authors of these three reports [1, 4, 5] is thus that, although containment failure is thought to be unlikely or impossible, physical uncertainties have so far prevented this from being demonstrated. A number of other studies, however, have argued that these uncertainties are less important and that a small or zero probability can be adopted with certainty.

The Report of the Swedish Government Committee on Steam Explosions [6] advanced several arguments that containment failure is impossible and concludes that "it is possible to exclude completely the possibility of steam explosions of such force that they could lead to rupture of the reactor vessel and containment."

Fauske and Associates, Inc. have argued [7] that large steam explosions are impossible at ambient pressures near to atmospheric because steam production would prevent formation of a large enough coarse premixture; and at higher pressures because triggering will not occur. They conclude that containment failure by this mechanism is impossible. Similar arguments have been advanced by Theofanous and Saito [8, 9] who conclude that "the steam explosion-induced containment failure probability is judged essentially incredible, i.e., at least two orders-ofmagnitude lower than the 10^{-2} estimate given in WASH-1400."

Mayinger [10] argued that molten core flows slowly out from a degraded core so that steam explosions involving a large amount of melt cannot occur in a reactor, and that even if such an explosion did occur, so small a percentage of the heat in the melt would be converted into kinetic energy as to preclude endangering either the reactor pressure vessel or containment building.

Squarer and Leverett [12] assigned the following probabilities in an event tree:

probability of large coherent melt mass, given core melt	10^{-1}
probability of presence of subcooled water	10^{-1}
probability of containment failure, given large melt mass and subcooled water	10^{-2}

Taken together these give 10^{-4} for the probability of containment failure, given a core melt accident. Despite acknowledging some phenomenological uncertainty, Squarer did not estimate the uncertainty in his probability.

1.3 Aims of this Report

Two points of view are summarized in Subsection 1.2; that our understanding of the physics of steam explosions and their effects is, or is not, sufficiently certain to justify the conclusion that containment failure is impossible or very unlikely.

Although conflict can arise over single estimates of the probability of containment failure, we are more concerned here with different perceptions of the degree of the uncertainty of this probability. Resolution of the conflict concerning uncertainty lies in a proper clarification of the combination of the various component uncertainties into an expression of the overall uncertainty. This report attempts such a clarification and resolution.

This report therefore has two aims: The first is to provide an uncertainty estimate for the conditional probability of containment failure by steam explosions (given core melt). The second is to identify important contributors to this uncertainty, in order to provide understanding of the reasons for its magnitude and to indicate what additional information would be needed to reduce it.

This report offers several improvements over a previous analysis of this problem by Swenson and Corradini [11]. The uncertainty is evaluated in a more complete and systematic manner. Also, modeling changes have been made. One modeling change that influences the results strongly is that a more realistic, and lower, limit is placed upon the capability of the upper internal structure within the reactor pressure vessel to dissipate explosive energy. Other changes were made in several of the assumed input distributions, including those describing the amount of melt that participates in an explosion and the fraction of thermal energy converted to mechanical energy (conversion ratio).

2. Methods

2.1 Uncertainty and Sensitivity Analysis

We first distinguish between uncertainty and sensitivity analysis. Uncertainty is a state of incomplete knowledge, and our uncertainty of the value of a quantity is expressed as the range within which we are reasonably sure that it lies. Uncertainty analysis is the process of determining this range, and this can be accomplished by finding the smallest and largest values of the quantity of interest that are obtained by varying the parameters upon which it depends over their ranges of uncertainty.

The sensitivity, S_i, of dependent variable F to a change in one of the independent variables, x_i, can be defined as

$$S_i \equiv \frac{\partial F(x_1, x_2, \ldots)}{\partial x_i}$$

Hence, a change in the function F, i.e., δF_i, which results from a small change in the independent variable x_i, i.e., δx_i, is given by

$$\delta F_i = S_i \, \delta x_i$$

However, sensitivity is used here in a more general sense, to include the effect of changes in F when the underlying variables are varied over their ranges of uncertainty.

This study incorporates both uncertainty analysis and sensitivity analysis to attain the aims set out in Subsection 1.3. The sensitivity study will identify the important factors contributing to the overall uncertainty.

2.2 Monte Carlo Method

The earlier study [11] used a simple parametric model of a steam explosion and its effects which determined whether or not containment failure occurred as a function of values of uncertain parameters (such as fraction of core molten and conversion ratio). The uncertain parameters were sampled by the Monte Carlo method. In this method probability density distributions are assigned to each uncertain parameter. A value for each parameter is sampled at random according to these distributions. The model then determines whether containment failure occurs. Such trials are repeated many times, each time with a newly sampled set of parameters. The fraction of trials in which containment failure occurs is then an estimate of the probability of failure.

The uncertain parameters used in reference 11 and in this study have the following features in common:

1) Each parameter is known (with greater or lesser certainty) to lie within an interval bounded by values based on physical arguments.

2) It is not known whether each parameter takes the same value (or range of values) for different accident sequences.

3) It is not known whether each parameter takes the same value for hypothetically repeated occurrences of the same accident sequence. Some may well do so but others, being random variables, may not.

4) If there are parameters which take different values for hypothetical repetitions of the same accident sequence, their probability distributions (conditional on accident sequence) are unknown.

In these circumstances, if probability distributions are assigned to the uncertain parameters, they must be interpreted as distributions of subjective probability for consistency in calculations. The concept of subjective probability has been extensively discussed in textbooks; the points required for this study are summarized in Appendix A.

For consistency of method with the previous study [11], this study uses Monte Carlo sampling of subjective probability distributions of the parameters that the previous study found to be important. As explained in Appendix A it is necessary to vary these distributions, within their possible ranges. Each subjective probability distribution is therefore systematically varied within the range of its parameter. A complete variation of such a distribution would include distributions of all possible shapes, widths and means. The selection made here is of three flat distributions covering the high, middle and low thirds of each parameter range. Evidence does not exist to determine the choice of distributions used, so it is essentially arbitrary. The present choice of rectangular distributions was made because these distributions cover the whole parameter ranges used, they allow sampling from different parts of the ranges separately, they avoid giving the erroneous impression that they are derived from direct measurements, and they do not express any preference for different parts of the ranges. Other choices of distributions could equally well have been used, however. Subsection 5.5 below discusses the effect of this choice upon the conclusions of this study. The numerical results show that the selection of distributions used did not cause underestimation of the uncertainty in the containment failure probability. This selection also cannot cause overestimation of the uncertainty because it is only a subset of the possible distributions.

The probability of containment failure due to in-vessel steam explosions may depend on the accident sequence. Thus, with complete knowledge, the probability could be evaluated for each sequence; if desired, a weighted average could then be obtained for all sequences or a subset of them.

The calculations in this report refer to an unspecified sequence where the ambient pressure is near to atmospheric with water in the vessel. The same uncertainty intervals for the uncertain parameters apply for each such sequence. Thus our calculated uncertainty interval for the probability of containment failure will encompass the values corresponding to each of the above-mentioned sequences and their weighted average. The fraction of core-melt sequences having no water in the vessel is unknown but it could be zero. Including such sequences, in which steam explosions cannot occur, would reduce the weighted average probability. Anticipating results obtained later in this document, the calculated range of containment failure probabilities includes the value zero. Thus our calculated uncertainty interval will also apply to the weighted average probability for all sequences near to atmospheric pressure.

Sections 5 and 6 discuss the effect of relaxing the restriction on pressure.

3. Modeling Assumptions

3.1 General

Section 3 describes the model of steam explosions and their effects used in this study. It indicates which parameters are uncertain and over what ranges, and the distributions and values that are sampled from these ranges.

The core-melting process is characterized by the fraction of the core molten at the time of the steam explosion (Subsection 3.2). This molten core is modeled as flowing out from the core region in a stream having a particular diameter; the melt mixes with residual water in the RPV lower plenum and after a delay, parameterized by the length of the pour, an explosion is triggered (Subsections 3.3 and 3.4). Subsection 3.5 discusses recently-proposed hypotheses that melt-water mixing is limited by steam production and concludes that while they are within the realm of possibility they have not yet been established well enough to justify an upper bound on mixing. The quantity of the available water that is in the mixture is deduced from current data (Subsection 3.6).

When a steam explosion occurs, a certain fraction of the heat "available" in the hot melt, i.e., of that in excess of the temperature of the water, is converted into kinetic energy. This fraction is called the conversion ratio; appropriate values of this are discussed in Subsection 3.7. Subsection 3.8 discusses the heat content of the hot melt.

The kinetic energy produced in an explosion is shared among the materials thrown off. In the present case the geometrical arrangement of melt and water immediately prior to the explosion affects the partition of this energy (Subsections 3.9 and 3.10). This partition is also affected by whether or not the RPV fails at the bottom; this can mitigate the effects of a steam explosion upon the top of the vessel by venting explosion products and kinetic energy downwards (Section 3.11).

The destructive potential of the upward-moving slug of material driven by the explosion depends on its density as well as its energy (a denser slug of the same mass and energy will exert a higher pressure on an obstacle it encounters). The slug density depends on its composition including any voids within it (Subsection 3.12).

As the slug traverses the upper internal structure (UIS) above the core region in the RPV it may damage it and be decelerated by it (Subsection 3.13). If the UIS does not stop the slug, the slug next impinges on the vessel top head. The resulting pressure loadings are discussed in Subsection 3.14, together with the criterion for failure of the bolts retaining the top head and consequent missile generation.

If a missile is generated, it may be stopped by a missile shield. Alternatively the shield will reduce the missile energy. The missile energy will be further reduced by gravity. The missile may then hit the containment dome and, depending on its speed at impact, fail it (Subsection 3.15).

Subsection 3.16 summarizes the modeling described in Section 3 by listing the equations used.

This study only considers pressurized water reactors. Physical dimensions have, where possible, been taken from the Zion plants, Units 1 and 2 [14]. The results should not be assumed to apply to other PWRs without a careful comparison of the important initial and boundary conditions. The calculations refer to accidents where the ambient pressure in the primary system is near to atmospheric. In Subsection 5.1 below, we describe the rationale for this constraint, and possible effects of relaxing it.

3.2 Fraction of Core Molten

This means the fraction of the reactor core molten at the time of the postulated steam explosion or, if more than one explosion occurs, at the time of the largest one. This quantity is determined by the processes of core degradation and the sequences of core degradation and melting which are at present not well understood. On the one hand it is argued [10] that melt issues steadily from a degraded core as soon as it is formed over a period of many minutes and therefore the fraction molten at the time of any explosion will be small (< 0.1%); on the other hand, the possibility remains that a self-heated pool of melt will be retained and held up by a crust of refrozen melt until a large fraction of the core has melted [2]. Thus our range for the fraction of core molten is 0.0 to 0.75. The higher value corresponds to the whole core except a layer 160 mm thick over the side, top and bottom; it is difficult (but not impossible) to envisage a larger melt pool than this. Subsection 4.3 describes a sensitivity study in which the effect of fractions of core molten in the range 0.75 to 1.0 was investigated. For the cases studied, these higher values made little difference; this is because the pouring parameters (Subsections 3.3 and 3.4) generally provide the strongest constraint on the mass of melt in an explosion. The total mass of fuel elements in the core is 125,200 kg, so 0.75 of this is 93,900 kg. Figure 1 shows three uniform probability distributions used for the fraction of core molten (low: 0-0.25%; middle: 0.25-0.5; and high: 0.5-0.75).

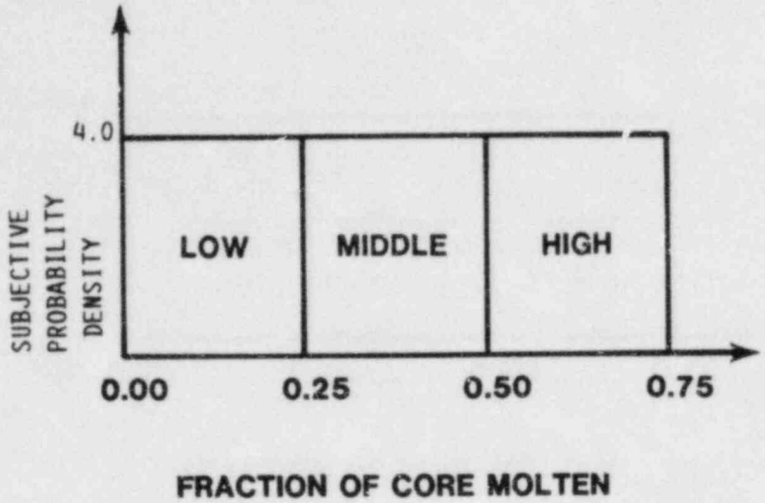

Figure 1: Three Uniform Distributions of Fraction of Core Molten

3.3 Pour Diameter

The quantity of molten core that mixes is parameterized here in a different way from that in the earlier study [11]. Instead of using the fraction of molten core that mixes, melt is assumed to pour out through a circular hole of constant diameter over a distance called the pour length before an explosion is triggered. The volume of melt participating in the explosion is the product of the area of the hole and the pour length.

The two ways melt can pour into the lower plenum are either downward penetration through the lower core plate (Figure 2), or sideways penetration of the melt through the baffle plate, core barrel and thermal shield (Figure 3). For failure of the lower core plate, the two conditions that limit the flow rate are the exit hole diameter and the flow area through the diffuser plate. The exit hole diameter will be determined by the size of the initial failure and any ablation as the pour proceeds. The 96 support columns provide redundant support of the lower core plate: thus initial local failure of the plate may well not lead

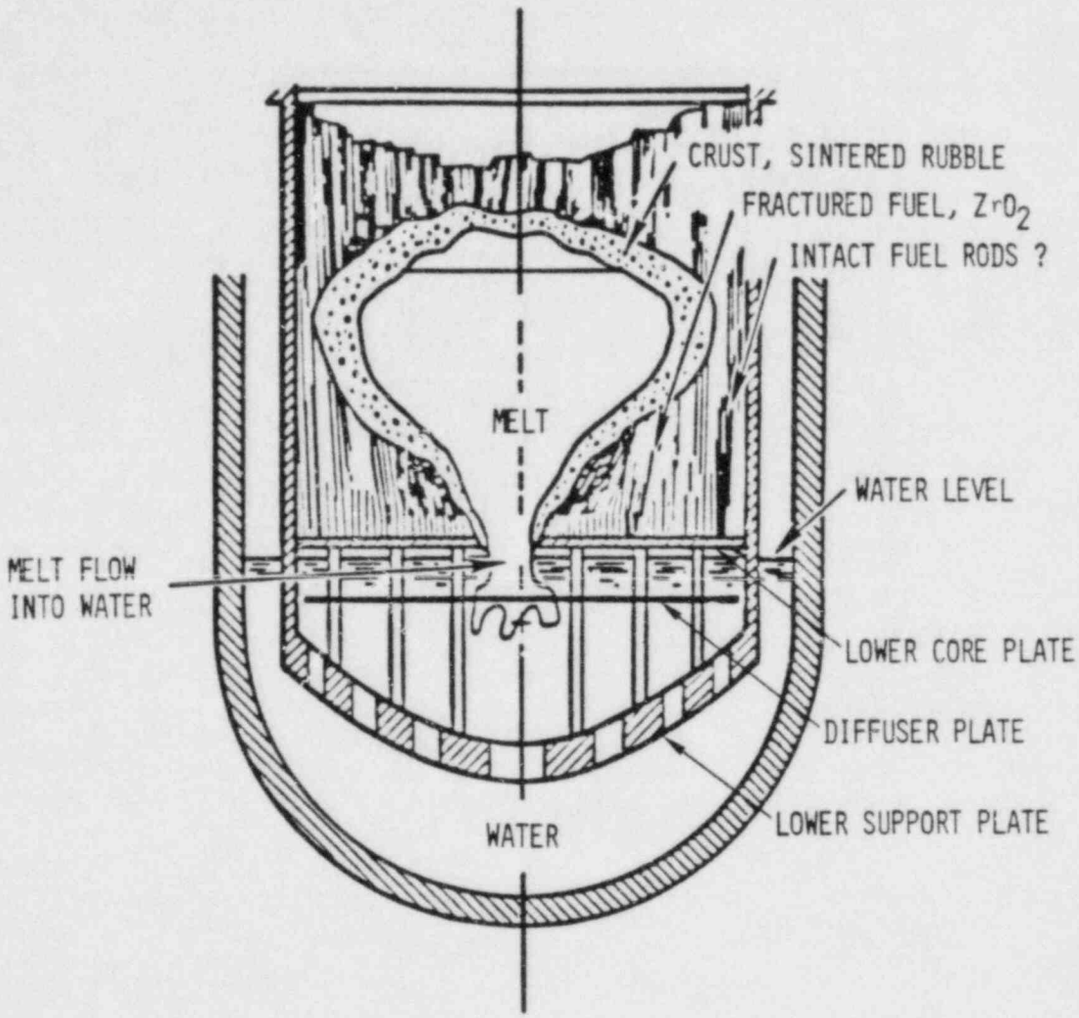

Figure 2: Melt Pour Into Lower Plenum by Failure of the Lower Core Plate

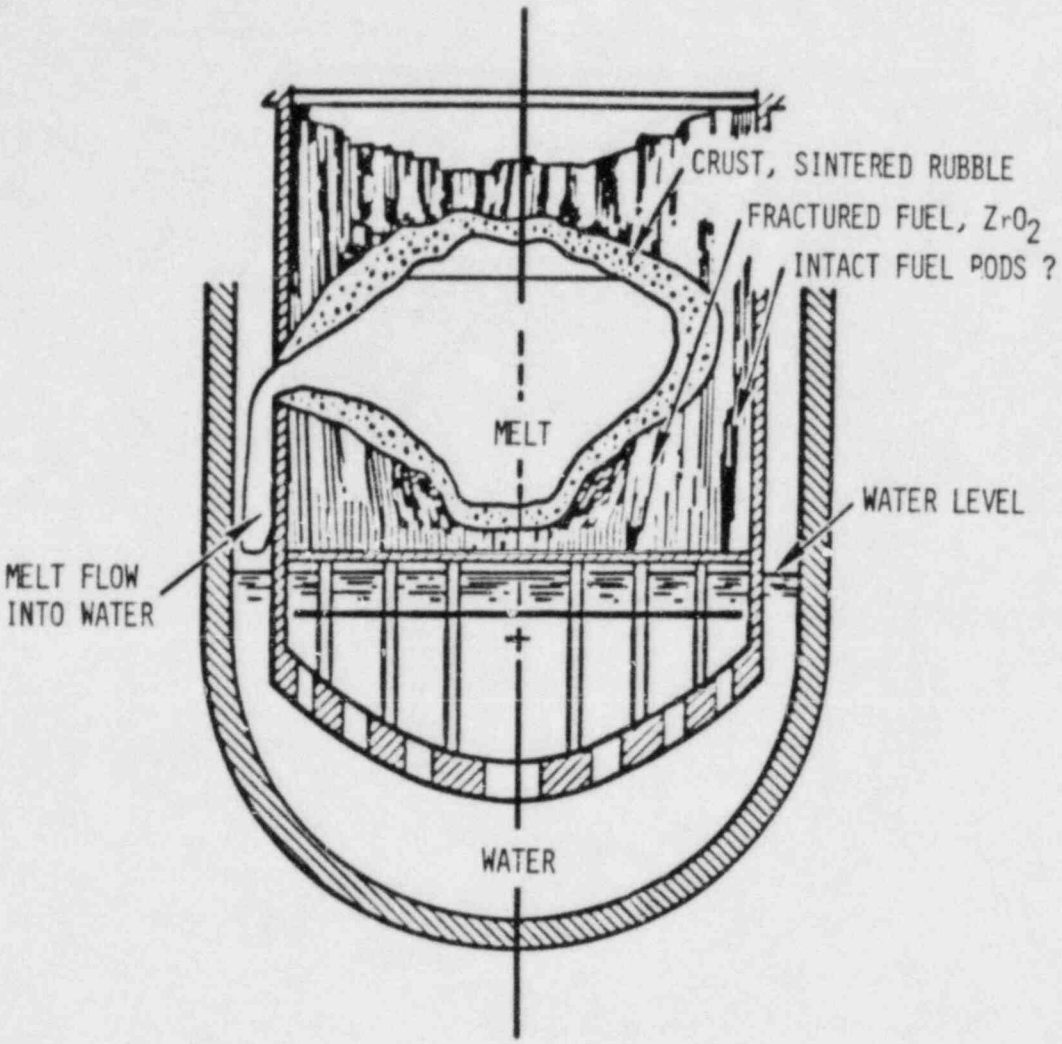

Figure 3: Melt Flow Into The Lower Plenum by Sideways Penetration of the Core Barrel

directly to a massive collapse. On the other hand an initial small pour may cause a steam explosion large enough to disrupt the lower core plate, causing a subsequent larger pour. Multiple explosions have frequently been observed in Sandia's steam explosion experiments [15, 16]. The second limiting flow area is the flow passages in the diffuser plate. If the lower core plate fails massively due to a steam explosion, the diffuser plate would probably be disrupted at the same time. If the diffuser plate remains intact the flow area would initially be limited by the open area in the diffuser plate - about 1/4 of the core area; this would lead to an estimate for pour diameter of 1/2 the core diameter. However the diffuser plate may be rapidly ablated, so this limitation on the pour diameter may not be effective.

Factors which can limit the effective pour diameter into the lower plenum due to sideways penetration include the size of the exit hole through the baffle, core barrel, and thermal shield, and the flow area available for the pour to enter the lower plenum by flowing down the downcomer. Because of the secondary core supports and the radial keys, it is unlikely that the entire circumference of the core barrel could fail simultaneously if the initial penetration is local. This will be the case unless melt progression is highly symmetrical. The size of the penetration will grow due to ablation, but the secondary supports will prevent the lower support structure from cocking and further opening the hole. The pour area is limited by the annulus between the core and the reactor vessel which, neglecting the thermal shield, is approximately 0.26 m wide. Assuming the pour occurs over 1/4 of the circumference leads to a flow area of 0.84 m^2. For the whole circumference it would be 3.4 m^2. Thus, the maximum flow area for sideways penetration and pouring is 3.4 m^2, corresponding to an effective diameter of about 0.3 of the core diameter.

The above arguments show that the upper limit of the effective pour diameter is the full core diameter. Hence, the distribution used for this parameter are those shown in Figure 4.

3.4 Pour Length (or Trigger Time)

Experimental data at intermediate scale indicate that a steam explosion can be spontaneously triggered at almost any time after melt entry into the water and up to about 30 ms after the mixture contacts the bottom of the vessel [16-18]. Furthermore, the melt front in the mixture appears to fall through the water with an approximately constant velocity [19, 20]. All the melt in the water at the time of triggering is assumed to be mixed and to participate in the explosion. This is consistent with the method used at Sandia to calculate conversion ratios, which employed the same assumptions. (Note that some experiments [21] have been analyzed by subdividing melt in the water into "mixed" and "unmixed" fractions). The possibility of limitations on the extent of mixing is discussed in subsection 3.5 below.

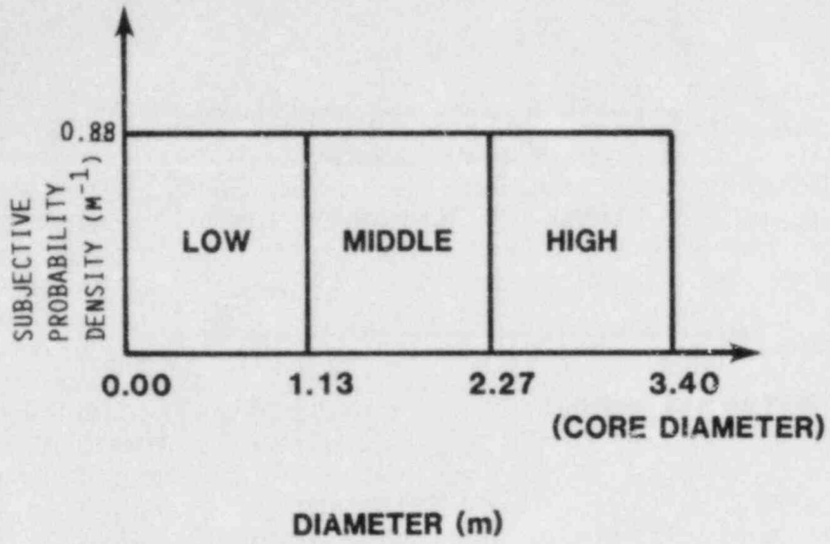

Figure 4: Three Uniform Distributions of Pour Diameter

In the reactor vessel, a likely trigger location would be the lower support plate, about 1.8 m below the core. It is also possible that the melt will pass through the support plate and be triggered at the bottom of the vessel, for example because the support plate may have been damaged or moved by the first of two steam explosions. Thus, the effective upper limit of the pour length is the depth to the bottom of the vessel, 3.0 m. The probability distributions used for this parameter are shown in Figure 5. Thus, the middle distribution includes the case where triggering occurs preferentially at the lower core support plate. The high distribution corresponds to triggering at the vessel base. Recent experimental data indicate that the ease of triggering of melt-coolant mixtures may increase with increasing scale [18]; i.e., larger masses might tend to be triggered at shallower depths. The low distribution allows for this possibility.

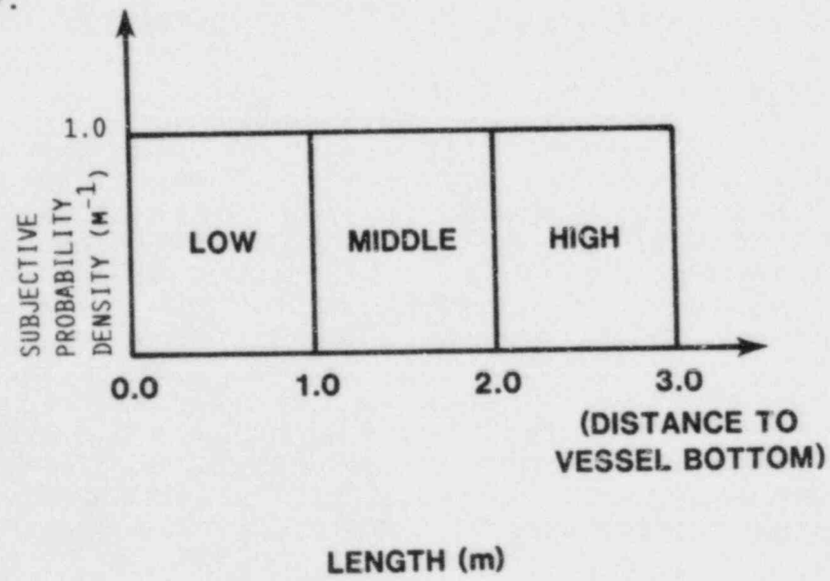

Figure 5: Three Uniform Distributions of Pour Length

Squarer has suggested that the water has to be subcooled for spontaneous triggering of an explosion [12]. This idea is called into question by two explosions observed in one test with saturated water by Buxton and Benedick [15] and by three spontaneously triggered explosions observed by Krein and Berman with hot water (subcooling only 2-5K) [22-24].

3.5 Mixing Limitations

The volume of melt participating in the explosion is assumed to be the product of the area of the pour and the pour length, or the total volume of the core molten, whichever is the smaller. The mass of melt is calculated using a density of 7000 kg/m^3. Table I indicates the ranges in melt mass available that result from grouping the various distributions together. For low distributions, the largest mass that could be mixed is 7000 kg. For the middle distributions, the mass range is 7000-56000 kg. For the high distributions, the range is 56000 to 94000 kg. The upper limit of 94000 kg corresponds to 0.75 of the core and is also the maximum that was used in the previous study [11].

TABLE I - RANGES OF POURED MASS

	Core Molten (1000 kg)	Pour Diameter (m)	Pour Area (m^2)	Pour Length (m)	Pour Volume (m^3)	Pour Mass (1000 kg)
Low	0-31	0.0 -1.13	0.0-1.0	0.0-1.0	0.0-1.0	0-7
Middle	31-63	1.13-2.27	1.0-4.0	1.0-2.0	1.0-8.0	7-56
High	63-94	2.27-3.40	4.0-9.1	2.0-3.0	8.0-13.4*	56-94*

*Limited by mass of core molten

It has been suggested [7, 8] that large coarse mixtures of liquid fuel and water cannot form because the resulting steam production would drive the mixture apart. This would preclude steam explosions involving large quantities of melt. Where these arguments are developed quantitatively [7, 25], they depend strongly upon a number of simplifying assumptions, notably those of a steady state and one-dimensional flow pattern [5]. The Henry-Fauske model [7, 25] predicts that only a few hundred kilograms could mix in the lower plenum, and that this quantity is independent of water depth. Theofanous has postulated that 2-3% of the core would

represent the maximum mass that could mix in-vessel [8, 9]; this would correspond to 2500-3750 kg. The Corradini model [19, 20, 26-31] predicts that the amount mixed increases with water depth and with coarse particle size. The latest formulation of this model [30, 31] predicts mixing of 3000 to 5000 kg corresponding to particle diameters of 50 to 100 mm.

Because of the simplifying assumptions in each of the models, all of the predicted upper limits to the extent of mixing are uncertain. For example one assumption made by Henry and Fauske is that melt particle diameters less than 1 cm are necessary for a steam explosion. However, although there is a wealth of data indicating that mixtures of cm-sized particles can explode (for example reference 17) it has been suggested [8, 9] that much larger particles can also participate in steam explosions. Another assumption made by these models is to ignore the potential of steam flows to enhance mixing as well as to suppress it. Two recent experiments, in which initially stratified configurations with water on melt exploded, demonstrated the possibility of such enhancement, because melt-water mixing appeared to take place spontaneously [23, 24, 32].

A complete mechanistic uncertainty analysis does not exist for any of these mixing models. Two examples show that they can be very sensitive to changes in assumptions, however. Corradini [30, 31] showed that changing the limiting criterion in the Henry-Fauske model from a critical heat flux criterion to a fluidization criterion changed the maximum fuel mass mixed from 100 kg to 550-750 kg for 10 mm particles or 5300-12000 kg for 100 mm particles. The ranges given in each case are due to uncertainty in the effective water particle size for fluidization. The current Corradini model [30, 31] assumes that the melt is initially in a spherical configuration. If, as in some earlier formulations [26] it is assumed that a cylinder of the same diameter and having length equal to the water depth can mix, this changes the range of upper limits from 3000-5000 kg to 14000-20000 kg.

These variations, although they cause large changes in model predictions, by no means take account of all uncertainties or span the whole range of possible mixing limitations. Corradini's model is the most detailed. It allows for transient break-up of the melt [29-31]; however the formulation used for this process is itself uncertain. None of the models allows for the possibility of the transient existence of mixtures which would be unstable due to large steam flows in a steady state. An extreme, but often observed, transient mixture of this kind is that formed by the first of two explosions.

Direct experimental evidence is inconclusive in distinguishing between large-scale mixing models because the bulk of the world's data was taken for melts of mass about 20 kg or less and is consistent with all proposed limits to mixing. Some recent

experimental data [33, 34] imply that the Fauske [25] model may underestimate the size of the mixtures that can be formed, but this has not been conclusively demonstrated.

Regardless of the accuracy of any of the models, there may well be a tendency for mixing to become more difficult with increasing scale. This could strongly influence failure probabilities. However, at present, evidence does not exist to allow an upper limit to be imposed on the mass of melt mixed that is less than all the available melt. The distributions used in this study effectively cover the whole range of possibilities. As shown in Table I, combinations of distributions that include "low" pour diameter or length allow for the possibility of very small amounts of coarse mixing. In addition, the maximum value in the low range is less than twice the Theofanous estimate of a maximum of 3,800 kg [8]. The uncertainties in the current coarse mixing models do not preclude any of the distributions studied here.

3.6 Fraction of Water That Mixes

The zones of mixed fuel, water and steam in the FITS experiments were observed to be roughly paraboloidal [17]. The data for the volume and depth of the mixing zones [19, 20] show that the diameter of the mixing zone tends to about four times the initial fuel diameter. The mixing zones contain 40-60% by volume of liquid water. Here we estimate the water mass mixed by assuming a cylindrical mixing zone with four times the diameter of the pour diameter. Thus, the masses of melt and water are approximately equal. For this analysis, the mass of water that mixes is set equal to the fuel mass or the total water mass (28000 kg), whichever is smaller. In these calculations, this mass only affects the partition of material between upward and downward moving slugs. A sensitivity study, described in Subsection 4.3, showed that the results were insensitive to changes in this partition.

3.7 Conversion Ratio

By conversion ratio, we mean the fraction of the heat in the melt participating in the explosion (assumed to be all the melt that mixes with water) above the water temperature, that is converted to kinetic energy.

Various estimates of the conversion ratios in reactor accidents have been made. Mayinger [6, 10] and Becker [6] refer to a report by Haag and Korber [35] which suggests that conversion ratio falls with increasing melt mass. This conclusion appears to arise from limited experimental data. Squarer [12] predicts conversion ratios of 1% or less. Theofanous and Saito [8, 9] estimate an explosion energy of 600 MJ which, together with their estimates of the mass mixed and of the heat in the molten core, implies a conversion ratio of 15%. Ultimately they expect that it will be possible to demonstrate a reduction of a factor of 5 from the

value, giving 3%. The Gittus Report [5] similarly estimates an upper limit of 4% subject to a factor of 4 uncertainty either way.

In the Zion/Indian Point study [3], calculations indicated the potential for a significant increase in conversion ratio with increasing scale. When an overlying molten pool was assumed to exist, steam expanding away from the explosion was further heated in passing through the molten region. Effective conversion ratios as high as 14% were calculated, much higher than the experimentally measured results discussed below. The difference was due to the calculated heating of the steam, compared to experiments where the steam is cooled by expanding through cold water, and possibly also due to increased inertial confinement. The predictions of these calculations however, are uncertain because of several simplifying assumptions used [5,6]. However they do indicate effects that should be taken into account when assessing the uncertainty introduced in extrapolating to larger scales.

Many experiments have been conducted at Sandia over the last few years to measure conversion ratios. Fifty-nine intermediatescale (< 20 kg) experiments were conducted in a cylindrical steel tank using iron-alumina and corium melts [15, 36]. The largest conversion ratio measured was 1.34% when a cover plate was used to increase the degree of confinement. In one other test, the conversion ratio was estimated to be nearly 1%. For the other 57 tests, it was 0.6% or less. Fifty-five tests have been conducted in the FITS and EXO-FITS facilities using corium and iron-alumina melts ranging from 1 to 20 kg [16, 17]. The largest conversion ratio measured was about 2.5%; as with the earlier tests, many of the explosions resulted in conversion ratios in the range of 1 to 2%. The relevance of these experiments has been questioned by Fauske and Henry [37]. Their criticisms have been answered by Corradini and Berman [23, 24]. The largest conversion ratio ever measured at Sandia National Laboratories was about 4.4% for a single-droplet explosion at an ambient pressure of 0.96 MPa [26, 38]. The accuracy of all these conversion ratio measurements is probably better than a factor of two.

Guided by these data, the range of conversion ratios from 0 to 5% was used for most of the calculations in this study, Figure 6. This range does not, however, fully account for the uncertainty introduced by extrapolating from kilogram-scale experiments to accidents at the scale of thousands of kilograms. At larger scales the conversion ratios may decrease as suggested by Haag and Korber, remain within the range currently observed, or increase (perhaps due to increased inertial confinement). Estimates of the largest conversion ratios possible may be made by considering calculations of maximum work thermodynamically possible. Such calculations have been made by Corradini and Swenson [11, 39] and by McFarlane [40]. Both of these assume that stated masses of molten core and water mix and come to thermal equilibrium at constant volume and then, with no further

heat transfer, expand up to the volume of the reactor vessel. The two calculations differ mainly in that Corradini and Swenson assume that the initial state has a 50% volume fraction of steam, while McFarlane does not. Table II gives the results of these two calculations. Corradini and Swenson predict lower maximum conversion ratios because their mixtures expand from larger volumes. Based on these calculations, we choose 16% as a representative upper bound on the conversion ratio. This value is also consistent with the upper limits of references 5 and 8. Additional flat distributions over the lower, middle and upper thirds of the range 0-16% were used to examine the sensitivity of the results of the study to the possibility that conversion ratio increases with scale.

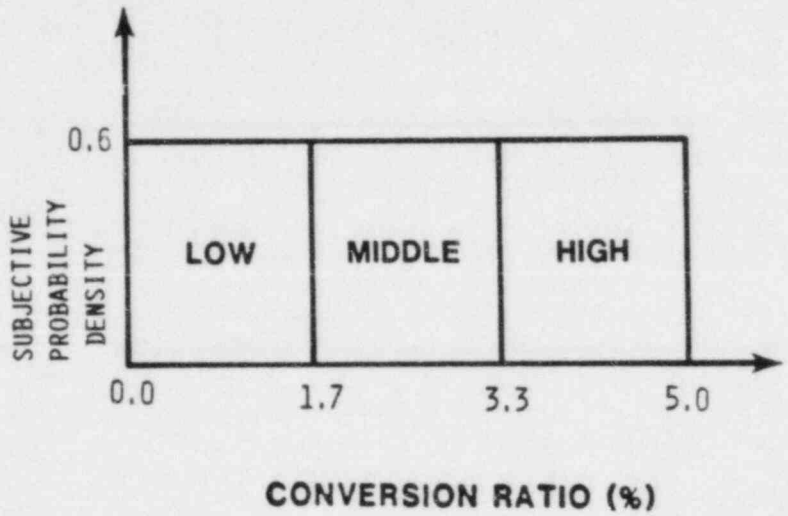

Figure 6: Three Uniform Distributions of Conversion Ratio

TABLE II. Thermodynamic Maximum Conversion Ratios (%)

Mass of Fuel (1000 kg)	Mass of Water (1000 kg)					
	5 Ref 39	5 Ref 40	10 Ref 39	10 Ref 40	20 Ref 39	20 Ref 40
5	13.1	13.2	4.8	6.3	3.8	2.3
10	15.9	19.3	9.3	10.3	2.7	4.6
20	17.9	22.2	11.4	15.9	6.3	5.3
40	10.7	16.9	12.8	19.2	8.0	13.2
80	7.3	10.9	7.6	16.2	7.0	16.9

3.8 Heat Content of Molten Fuel

The heat content of the molten fuel depends on the course of melt progression and the constituents of the melt. Because of uncertainty in core melt progression, the heat content is uncertain. In this study, we have assumed a base water temperature of 400 K. The lowest temperature at which core material may liquefy can be estimated at 2000 K, when liquid Zircaloy begins to dissolve solid UO_2. Using a specific heat of 500 J/kg-K for solid UO_2, and neglecting a small contribution from the latent heat of Zircaloy, gives 0.8 MJ/kg in the melt over 400 K as an estimate of the lower limit of the melt's heat content. An upper limit can be estimated by considering UO_2 heated up to its melting point, approximately 3100 K, and then melted with latent heat 0.27 MJ/kg. This implies a total latent plus sensible heat above 400 K of 1.6 MJ/kg. For most of this study the single value of 1.2 MJ/kg is used for the melt heat content; a sensitivity study investigates the effect of the values 0.8 and 1.6 MJ/kg as well.

The kinetic energy produced in the explosion is the product of the mass of melt in the water at time of triggering, the heat content of the melt, and the conversion ratio.

3.9 Fraction of Remaining Melt Above Explosion

For calculations of events after the explosion we need to know the position of the melt that did not participate. In the previous study [11] the fraction of the remaining melt above the explosion was regarded as an undetermined parameter in the range 0.0 to 1.0, the rest of the melt was assumed to be below the explosion.

For simplicity, we have assumed that all the melt that did not participate in the explosion remains above the explosion in most of the calculations in this study. Alternative assumptions used are discussed in Subsection 3.10.

3.10 Fraction of Remaining Water Above Explosion

Similarly to their treatment of remaining melt, Swenson and Corradini [11] assumed that, of the water not participating in the explosion, a fraction between 0.0 and 1.0 could be located above the explosion. As in [11], we assume that all the water not participating in the explosion lies below the explosion for most calculations.

Both the assumptions in this Subsection and Subsection 3.9 may not be right; but they counteract one another in determining the slug energy and so do not represent an extreme combination. The possible extreme combinations in which all the melt and all the water not participating in the explosion are either both above or

both below the explosion are investigated in a sensitivity analysis discussed in Subsection 4.3. This shows the results to be insensitive to these assumptions.

3.11 Energy Dissipation by Bottom Failure

In common with the previous analysis [11] we assume that the base of the RPV fails if the explosion energy exceeds 1000 MJ. Reference 3 placed this threshold in the range 1000 to 1500 MJ.

In Subsection 4.3, a sensitivity study shows that the results are insensitive to the value of this threshold within the range 500 to 1500 MJ.

Swenson and Corradini [11] assumed that failure caused dissipation of between 0.0 and 0.5 of the explosive energy: the remainder being kinetic energy of the upward moving slug. Here we assume that, if the bottom of the vessel fails, two masses are accelerated: a downward moving one consisting of the vessel base (30,000 kg), the water below the explosion and one-half of the water and melt participating in the explosion; and an upward moving slug being the other half of the melt and water in the explosion and the melt above the explosion. On the assumption that there is no net transfer of momentum from the body of the vessel to the slugs, these share the explosion kinetic energy in inverse proportion to their masses.

$$KE_{slug} = \frac{\text{mass below}}{\text{mass above + mass below}} \; KE_{explosion}$$

These simplifying assumptions neglect the delay before bottom failure (which would increase the upper slug's energy) and sideways venting of steam and work absorbed in failing the bottom (which would reduce it).

3.12 Slug Composition

If the vessel bottom does not fail the upward moving slug is assumed to consist of all of the melt and water participating in the explosion and the melt above the explosion. If the bottom does fail, only half of the exploding materials are assumed to move upwards.

Steam formed in the explosion may impregnate the upward moving slug with bubbles or break it up into a spray of droplets. This would change its mechanical effects by altering the momentum flux in the slug and hence its stagnation pressure.

We treat the volume fraction of condensed phases (liquid plus solid) in the slug as an uncertain parameter. On the one hand the volume fraction of condensed phases might be large, as steam might not penetrate forward into overlying melt, and might be

compressed during interaction between the slug and upper internal structure. We take 1.0 as an effective upper limit. As a lower limit we take a volume fraction of 0.25. Figure 7 shows the distributions of this parameter used.

In calculations of the effects of slug impact (Subsection 3.14) the slug density is calculated from the masses of water and fuel and volume fraction of steam in the slug.

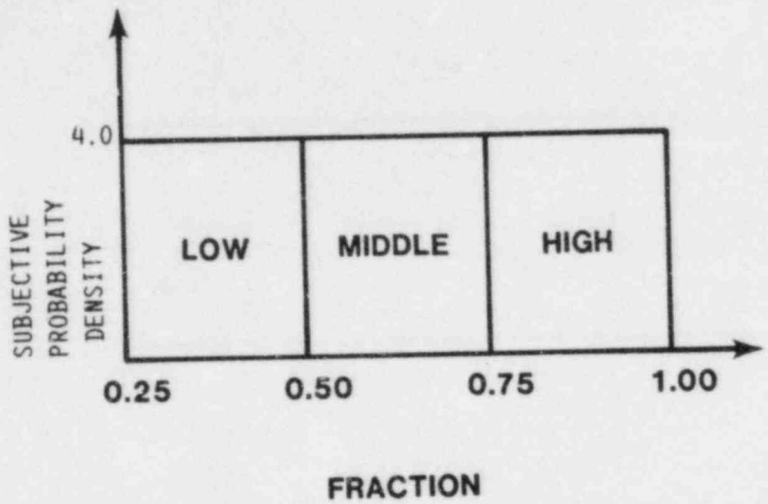

Figure 7. Three Uniform Distributions of Condensed-Phase Volume Fraction in Slug

$$\text{vol}_{\text{slug}} = \frac{\frac{\text{fuel mass}}{\text{fuel density}} + \frac{\text{water mass}}{\text{water density}}}{\text{volume fraction of condensed phases}}$$

$$\rho_{\text{slug}} = \frac{M_{\text{slug}}}{\text{vol}_{\text{slug}}}$$

3.13 Energy Dissipation by Core and Upper Internal Structure

The remains of the reactor core after a core-melt accident are unlikely to be able to withstand substantial forces and hence to be the cause of significant dissipation of energy following a large explosion. Effects of the order of the gravitational potential energy of the core, ~ 1 MJ, are to be expected but this is negligible in comparison with the explosion energies considered here. Thus we ignore absorption of slug kinetic energy in the residual core.

The space between the upper core plate (at the top of the core) and the upper support plate (at the level of the vessel flange) is 3.22 m high. It contains 48 support columns which hold the core down against hydraulic friction forces in normal operation, and control rod guide tubes and drive shafts and any control rods in the withdrawn position. The space above the core is needed to accommodate withdrawn control rods.

For our present purposes we call the components between the upper core plate and the upper support plate the "upper internal structure" (UIS). Interaction between a fluid slug and this structure will dissipate energy produced by a steam explosion [2, 11].

The extent of this dissipation is difficult to estimate because of the uncertain material properties of the slug and the transient nature of the slug loading and the structural response. Reference 11 assumed, by analogy with experiments in which water was forced through an undeformed scale model of the upper internal structure of a fast reactor, that the whole UIS would absorb 90% of the slug's kinetic energy; and that this factor would be proportionally reduced if part of the UIS had been melted away. Squarer proposes a similar formulation in which 75% of the kinetic energy is absorbed [12].

We retain the description in reference 11 here with two modifications. First, the UIS is assumed to be fully intact. This is because it might initially be protected from high temperatures and heat fluxes (radiative and convective) from the center of the degraded core by the upper layer of the core. However, recent calculations have demonstrated that, particularly in accident sequences in which the RCS pressure is high, convective heat transfer from the core can cause melting in the UIS before core melting begins [41]. The error introduced if the assumption that the RCS remains intact is wrong is small, as discussed at the end of this Subsection.

Second, the energy absorption in the UIS is limited by its capability to withstand the corresponding forces. These can be estimated simply and roughly. We assume the coupling between the slug and undeformed UIS can be described by a constant friction factor. Then the resultant retarding force exerted on the slug by the UIS will be proportional to its kinetic energy. This force, F, reduces the kinetic energy, E, as a function of distance traveled,

$$\frac{dE}{dx} = - F = - CE$$

$$E = E_u \, e^{-Cx}$$

Since E is presumed to fall by a factor of 10 over a distance 3.22 m (corresponding to absorption of 90% of the kinetic energy), C = 0.715 m^{-1}. Thus the restraining force on a slug of given energy can be estimated.

The force decelerating the slug is transmitted through the UIS to the upper support plate and thence to the RPV. We now roughly estimate the capacity of the UIS to transmit this force. Its only components designed to withstand forces in this direction are the 48 support columns. These are slotted steel tubes of outside diameter 190.5 mm and thickness 12.7 mm and total cross-sectional area, taking account of the slots, of 0.155 m^2. Assuming a yield stress of 468 MPa implies a maximum sustainable force of 72.5 MN. This will be a substantial overestimate of the average force during crushing because slight asymetries in plastic yielding will produce buckling which will be enhanced by the slots and will reduce the force required to collapse the columns. However it will be a better estimate of the force required to initiate crushing.

From the calculation of the frictional forces above, this crushing threshold corresponds to a slug energy of 101 MJ. Thus we presume the UIS to absorb 90% of the kinetic energy of slugs less energetic than this. More energetic slugs will be presumed to crush the UIS against a constant force of 72.5 MN (probably an overestimate as noted above) until their kinetic energy falls below 101 MJ. Thus the maximum energy absorbed is 233 MJ when this force acts over the whole length, 3.22 m, of the UIS, and this energy will be absorbed from the slugs of initial energy greater than 233 + 101 = 334 MJ. Slugs of intermediate energy will first be decelerated by a constant force and then an exponentially falling one, but for simplicity we interpolate the energy absorption linearly between the two extreme cases as shown in Figure 8.

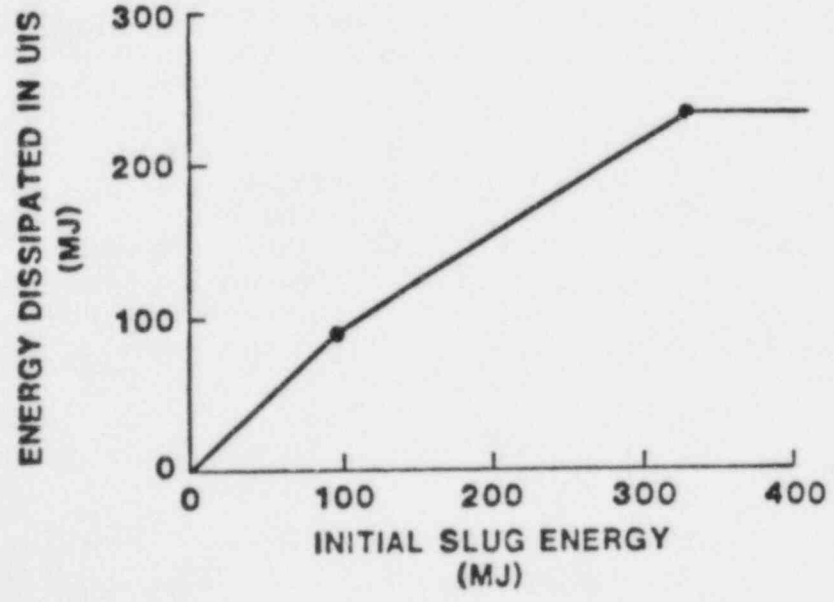

Figure 8: Energy Dissipation in Upper Internal Structure

Because of the possibilities that the UIS is weakened by heating and that its crushing strength is less than calculated here, the dissipation calculated is an upper bound. Since the greatest possible dissipation calculated, 233 MJ, is approximately a factor 10 smaller than the slug energy required to fail the vessel top head, extra uncertainty caused by overestimation of this dissipation will not be considered further.

3.14 Slug Impact Model

The six degree of freedom slug impact model described in Ref. 10 is one dimensional and hence less realistic than calculations [3, 4] which demonstrate the importance of two-dimensional effects. The slug exerts a pressure on the RPV top head of approximately ρuc where ρ is the slug density, u its speed and c its sound speed. This corresponds to the plane reflection of a sound wave of velocity u. Additionally the values of c used depend upon the particular prescription assumed for the speed of sound in a composite medium [11].

Instead here we approximate the pressure to be expected in two-dimensional flow, in which fluid moves up, across the vessel head and down again, by the stagnation pressure ρu^2. This is equal to the flux of momentum across a plane through which the slug passes. We take the total force on the RPV head to be this pressure multiplied by the cross-sectional area of the vessel, 14.1 m^2. Thus we assume that the part of the vessel's area not occupied by upward flowing material contains material flowing downwards whose acceleration makes a contribution to the total force on the head.

It may be that the upper support plate, which spans the vessel at the level of the top head flange and which is reinforced by a web of cross members, is strong enough to withstand the pressures exerted by the slug. This will not change our analysis because if this plate does not fail it transmits the force exerted on it directly to the upper head just above the bolts.

In Appendix B, we discuss some of the possible vessel failure modes resulting from slug impact. The most damaging failure would occur if the studs fractured and allowed the head to fly off. The criterion used in these calculations for failure of the top of the RPV is that the force on it exceeds the failure tension of the bolts. Multiplying their combined cross-sectional area, 1.341 m^2, by the failure stress of 870 MPa gives a total bolt failure tension of 1170 MN. Note that bolt fracture occurs while the bulk deformation is elastic, before plastic deformation of the bolts occurs.

As shown in Appendix B, the period of natural vibration of the vessel is short enough relative to the loading that the loading can be assumed to be static. We can then calculate the loading pressure and compare it to the failure pressure to evaluate vessel failure.

Subsection 5.2 discusses the effect of other possible failure modes of the top of the RPV.

3.15 Containment Failure

In this report, we are interested in containment failure resulting from impact by the head. The Zion containment structure is in the shape of a cylinder with a shallow, domed roof and a flat foundation slab. Some approximate dimensions of the reactor containment are: inside diameter 42.7 m; inside height 64 m; containment dome height above reactor 45 m; vertical wall thickness 1.07 m; and dome thickness 0.81 m. The entire structure is post-tensioned and lined with 6.35 mm-thick welded steel plate to provide vapor tightness.

In addition to the barrier provided by containment, a concrete missile barrier is positioned above the reactor vessel to block any missiles generated by the failure of the control rod housings. Approximate dimensions of the barrier are a radius of 2.5 m and a thickness of 1.3 m. The approximate mass is 65,000 kg. Other equipment above the missile shield includes the polar crane.

The sequence of events leading to hypothesized containment failure starts with failure of the studs, which allows the head to rise and impact the missile shield. Impact with the missile shield absorbs some of the head energy. The head then continues to rise and impacts containment. Some additional energy is then absorbed in breaching containment.

In this calculation, we have estimated the velocities to perforate the missile shield and containment using both the NDRC formula modified for low-speed impact [42, 43] and the CEA-EDF formula [44]. These perforation velocities then give the energy absorbed during these impacts. These formulae are listed in Table III. Alternately, we assumed that impact with the missile shield reduced the head velocity in half. This is equivalent to an inelastic collision between the head and shield assuming that a part of the shield, equal in mass to the head, continues to travel with head.

For missile shield perforation, the NDRC equation gives a required velocity of 39 m/s, while the CEA - EDF equation gives 55 m/s. For the containment, the NDRC equation gives a velocity of 23 m/s, while the CEA - EDF equation gives 29 m/s.

We now can calculate the range of possible required initial velocities for containment failure. For the smallest velocity, we assume the head perforates the missile shield with energy loss calculated by the NDRC formula and impacts the containment with a small velocity that nevertheless damages it. Summing the kinetic

Table III. Perforation Formulae [5]

Nomenclature:

d	missile diameter (m)
m	missile mass (kg)
ρ	concrete density (2400 kg/m^3)
σ_c	concrete compressive strength (28.6 X 10^6 Pa)
V	missile velocity (m/s)
x	target thickness (m)

Modified NDRC Formula [42, 43]:

$$G(Z) = 2.55 \times 10^{-9} K N d^{0.2} D V^{1.8}$$

$$K = \frac{1.49 \times 10^4}{\sqrt{\sigma_c}} = \text{Concrete Penetrability Factor}$$

$N = 1.0$ for spherical-nosed missile (dimensionless)

$$D = \frac{m}{d^3} \ (kg/m^3) = \text{Calibre density}$$

$$G(Z) = \left(\frac{x}{4d}\right)^2$$

CEA - EDF Formula [44]:

$$x = 0.82 \ \sigma_c^{-3/8} \ \rho^{-1/8} \ \frac{m}{d}^{1/2} \ V^{3/4}$$

$$20 < V < 200$$

$$0.3 < x/d < 4$$

energies absorbed in perforation and the gravitational potential energy needed to rise through 45 m gives a required initial velocity of 49 m/s. For the largest velocity, we assume first an inelastic collision between the head and missile shield in which the head loses 3/4 of its kinetic energy, and subsequent perforation of containment with energy loss calculated by the CEA-EDF formula. Then the required initial velocity is 83 m/sec. In Section 4, we tabulate missile velocities of 50 m/sec and 90 m/sec to include the range of these results. This range of missile velocities should not be regarded as a fully justified uncertainty interval because some extrapolation from the experimentally tested ranges of the correlations was used and because of the possibility of effects, such as spinning, which differ from the ideal vertical missile trajectory assumed.

3.16 Summary of Modeling

This subsection summarizes the modeling described in Section 3. First the meanings of the symbols used are listed. Then the equations defining the model are set out, with references to the Subsections where detailed discussion can be found.

Nomenclature:

A_b	total cross sectional area of bolts
A_v	cross sectional area inside vessel
d_p	pour diameter
E_b	threshold explosion energy for vessel bottom failure
E_d	slug energy dissipated in UIS
E_e	explosion energy
E_r	residual slug energy after dissipation in UIS
E_u	initial upward slug energy
E_1	initial kinetic energy of top head
E_2	kinetic energy of top head after missile shield impact
E_3	kinetic energy of top head at containment impact
F_c	volume fraction of condensed phases in slug
F_m	fraction of core molten
g	acceleration due to gravity
h	height from missile shield to containment dome
H	heat content of melt
l_p	pour length
M_b	mass of vessel base
M_c	mass of core
M_d	mass of downward-moving slug
M_h	mass of vessel top head
M_m	mass of melt mixed with water
M_p	mass of melt poured out from core
M_t	mass of water
M_u	mass of upward-moving slug
M_w	mass of water mixed with melt
P	pressure exerted by slug on top head
R	conversion ratio

ρ_m density of melt
ρ_u density of upward-moving slug
ρ_w density of water
σ_b failure stress of bolts
u velocity of slug at impact on top head
V_c volume of condensed phases in upward-moving slug
V_u volume of upward-moving slug

Mass of melt in explosion (Subsections 3.2 to 3.5):

$$M_m = \min\left(M_c F_m, \frac{\pi d_p^2 \, l_p \, \rho_m}{4}\right)$$

Mass of water in explosion (Subsection 3.6):

$$M_w = \min(M_t, M_m).$$

Energy of explosion (Subsections 3.7, 3.8):

$$E_e = M_m \, H \, R.$$

Condition for vessel bottom failure (Subsection 3.11):

$E_e > E_b \longrightarrow$ bottom failure.

Mass and volume of upward moving slug (Subsections 3.9 and 3.10):

	Vessel bottom intact	Vessel bottom failed
Water mass	M_w	$1/2\ M_w$
Melt mass	$M_c F_m$	$M_c F_m - 1/2\ M_m$
Total mass	$M_u = M_w + M_c F_m$	$M_u = 1/2\ M_w + M_c F_m - 1/2\ M_m$
Total volume (condensed phases)	$V_c = \frac{M_w}{\rho_w} + \frac{M_c F_m}{\rho_m}$	$V_c = \frac{\frac{1}{2} M_w}{\rho_w} + \frac{M_c F_m - \frac{1}{2} M_m}{\rho_m}$

(Different assumptions are used in a sensitivity study - Subsection 4.3)

Mass of downward moving slug if vessel bottom fails (Subsection 3.11):

Water mass	$M_t - 1/2\ M_w$
Melt mass	$1/2\ M_m$
Total mass	$M_d = M_t - 1/2\ M_w + 1/2\ M_m + M_b$

(Different assumptions are used in a sensitivity study - Subsection 4.3)

Kinetic energy of upward moving slug (Subsection 3.11):

$$E_u = \frac{M_d}{M_u + M_d} E_e.$$

Volume and density of upward moving slug (Subsection 3.12):

$$V_u = V_c/F_c$$

$$\rho_u = M_u/V_u$$

Energy dissipation in UIS (Subsection 3.13):

E_d depends on E_u as shown in Figure 8.

$$E_r = E_u - E_d$$

Impact velocity and pressure of upward moving slug (Subsection 3.14):

$$u = \left(\frac{2E_r}{M_u}\right)^{1/2}$$

$$P = \rho_u u^2$$

Condition for bolt failure (Subsection 3.14):

$P A_v > \sigma_b A_b \longrightarrow$ bolt failure

Initial kinetic energy of top head:

$$E_1 = \frac{1}{2} \frac{M_u M_h}{(M_u + M_h)} E_r$$

Energy reduction due to missile shield (Subsection 3.15):

Inelastic collision: $E_2 = 1/4\ E_1$

Penetration formula: $E_2 = E_1$ - kinetic energy needed to perforate

Condition for containment failure (Subsection 3.15):

$E_3 = E_2 - M_h\ g\ h$
$E_3 >$ kinetic energy needed to perforate $\longrightarrow$ failure.

4. Calculations and Results

4.1 Outline of Calculations

Subsection 1.3 of this report listed its aims. These are to provide an uncertainty estimate for the conditional probability of containment failure by steam explosions (given core melt) and to identify important contributors to this uncertainty. Subsection 2.1 explained that these aims would be attained by uncertainty analysis (to find bounds on the probability) and sensitivity analysis (examining the dependence of the probability on various samplings of the uncertain parameters, to determine which parameters have the greatest effect).

Section 3 described the uncertainties in modeling the various processes involved. Our modeling of these processes is relatively simple. Nevertheless, the number of different uncertain parameters in this simple model makes a fully comprehensive sensitivity study difficult. We have used one of many possible sampling schemes and selected calculations so that our conclusions are, as far as possible, independent of the particular cases studied. Since the selection of the sampling scheme used was essentially arbitrary, the reader is cautioned against attributing special significance to any individual calculated probability number. More attention should be given to the way in which the calculated probabilities depend upon the different parameters varied. Subsection 5.5 below discusses the effect of an arbitrary choice of a sampling scheme upon the validity of the conclusions that we draw.

As explained in subsection 2.2, it was desired to use a Monte Carlo sampling technique (with an adequate sample size) in order to make explicitly clear that any differences between the results of this study and the previous Monte Carlo study [11] were not due to a difference in statistical method. The five uncertain parameters judged to have the most important influence on the overall uncertainty were sampled by the Monte Carlo method as described in subsection 2.2.

These five parameters are called here the "first set." The first set parameters are the two found to be important in the previous study [11], conversion ratio and slug condensed phase volume fraction; and the three parameters which determine the amount of melt participating in a steam explosion, namely the fraction of core molten and the pour diameter and length. The importance of the amount of melt in the explosion is potentially high but it was not explicitly investigated in reference 11. The remaining parameters are called the "second set."

For each of the first set parameters, three alternative flat distributions of subjective probability were assigned covering the low, middle and high thirds of the uncertainty range of the

parameter. In the main study different combinations of these distributions were selected systematically as set out in Table IV. Single values of the second set parameters were used.

The second set parameters were the heat content of the melt, the location of melt and water not participating in the explosion, and the explosion energy required to fail the vessel base. As well as these parameters, three upper limits of first set parameters were varied in additional calculations: fraction of core melted, conversion ratio and pour diameter.

The second set parameters were varied over their ranges of uncertainties in additional calculations in which one or two additional single values of them, selected to cover their ranges, were used. Each of these values was combined with all the low, all the middle and all the high distributions of the first set parameters. This sampling thus spans the whole range of each of the first set parameters. These additional calculations are set out in Table V. They show that the second set parameters generally had, as expected, less important uncertainties than the first set parameters.

4.2 Results of Main Calculations

In these calculations the different distributions of the first set parameters were combined while keeping the second set constant at the following values:

Melt heat content: 1.2 MJ/kg
Position of unmixed melt: over explosion
Position of unmixed water: under explosion
Explosion energy needed to fail vessel base: 1000 MJ

The cases calculated and the results obtained are set out in Table IV. The entries in the Table are now explained, using Case 1 as an example. In this case each of the first set parameters was given a flat distribution of subjective probability, over its whole range. These full ranges are

Fraction of core molten:	0 - 75%
Pour diameter:	0 - 3.4 m
Pour length:	0 - 3.0 m
Slug condensed phase fraction:	25 - 100%
Conversion ratio:	0 - 5%

For all cases other than Case 1 distributions labelled L, M and H are used for these parameters. These mean

L:	flat, low third of whole range
M:	flat, middle third of whole range
H:	flat, high third of whole range.

TABLE IV. Main Calculations

		INPUT					CALCULATIONS				FAILURES (per 10,000 trials)			
	Case	Fraction Molten %	Pour Diameter (m)	Pour Length (m)	Slug* Condensed Phase Fraction (%)	Conversion Ratio (%)	Mean Explosion Energy (MJ)	Mean Slug* Impact Energy (MJ)	Mean Slug* Volume (m^3)	Mean Slug* Mass (1000 kg)	Vessel Bottom	Bolts	Large Missile V>50 m/s	Large Missile V>90 m/s
Full width	1	0-75	0.0-3.4	0.0-3.0	25-100	0-5	584	283	31.5	53.1	2017	466	460	267
All low	2	L(0-25)	L(0.0-1.13)	L(0.-1.)	L(25-50)	L(0.0-1.7)	11	1	9.3	16.7	0	0	0	0
All middle	3	M(25-50)	M(1.13-2.27)	M(1.-2.)	M(50-75)	M(1.7-3.3)	732	400	40.2	61.6	2126	1	1	0
All high	4	H(50-75)	H(2.27-3.4)	H(2.-3.)	H(75-100)	H(3.3-5.0)	3828	2088	22.6	53.8	10000	9987	9987	9959
All	5	L	M	M	M	M	407	211	25.2	28.6	172	0	0	0
Middle	6		L				106	24	16.6	50.3	0	0	0	0
Except	7			L			247	98	24.2	55.1	4	0	0	0
Indiv.	8				L		735	404	69.3	62.0	2087	0	0	0
Low	9					L	248	100	45.8	68.5	5	0	0	0
All	10	H	M	M	M	M	735	364	47.3	92.6	2136	0	0	.0
Middle	11		H				1352	683	32.9	43.8	8272	185	185	2
Except	12			H			1078	570	39.0	54.3	5335	62	62	0
Indiv.	13				H		722	396	28.8	62.1	1977	68	68	0
High	14					H	1203	595	31.3	51.8	5884	384	384	84
All	15	L	H	H	H	H	779	434	14.6	22.3	3479	1719	1557	0
High	16		L				293	147	19.5	84.0	79	0	0	0
Except	17			L			1116	433	25.1	81.5	5155	460	460	162
Indiv.	18				L		3820	2093	54.6	53.8	10000	4110	4110	4110
Low	19					L	780	392	37.2	87.4	3524	5	5	0
All Low	20	H	L	L	L	L	12	1	34.2	79.4	0	0	0	0
Except	21		H				118	31	38.5	27.3	0	0	0	0
Indiv.	22			H			49	8	19.8	20.5	0	0	0	0
High	23				H		11	1	3.8	16.7	0	0	0	0
	24					H	56	9	9.3	16.7	0	0	0	0

*Upward moving slug.

The distributions used in each case are listed in the five columns under "INPUT." In the text these distributions are referred to as "low," middle" and "high."

The next four columns give the mean values, out of 10000 trials randomly sampled from these distributions, of four calculated parameters. These are the mean steam explosion energy, the slug impact energy, and the volume and mass of the slug. Thus in Case 1 the mean steam explosion energy was 584 MJ.

The last four columns in Table IV give the number of failures of different kinds calculated to occur out of 10000 trials. Vessel bottom failures are listed first followed by failures of the top head retaining bolts. The last two columns give the number of containment failures if the threshold values for the initial velocity of the top head to cause containment failure is 50 or 90 m/s. This estimate of the uncertainty range for this parameter was calculated in Subsection 3.15. Thus the numbers in these two columns, divided by 10000, estimate the range of containment failure probability, conditional on the input distributions listed under "INPUT" and the values of the second set parameters listed above.

Caution should be used when the numbers in the last four columns are small, as they are subject to a sampling error approximated by their square roots.

Cases 2, 3 and 4 group all the low, middle and high distributions. The low distributions cause no failures. The middle distributions give 2126 base failures, and one bolt failure leading to a large missile with velocity greater than 50 m/s and less than 90 m/s. This result is very similar to the nominal PWR1 case of Reference 11 which gave 26% base failures and no bolt failures. This is coincidental because of the different assumptions used. The Case 3 result however differs from Case 1, in which the input distributions have the same means but larger widths. Case 1 permits parameter combinations leading to larger explosions than the largest possible in Case 3, and so leads to more vessel top and containment failures. Case 4, grouping all the high distributions gives 10000 base failures, 9987 bolt failure and 9959 with missile velocity greater than 90 m/s. The sharp rise in failure probabilities between Cases 3 and 4 is at first sight surprising as it appears to indicate a chance coincidence of a threshold with the boundary chosen between these cases (this boundary corresponds to an explosion of energy 2218 MJ). However it should be noted that the explosion energy is less densely sampled near its extreme values in each case because these extremes correspond to the coincidence of extremes in pour diameter, pour length and conversion ratio. As indicated in Section 3, all these distributions are within the bounds of possibility. So also are all their combinations. Since these combinations cover such a wide range of calculated probabilities it is necessary to investigate further combinations to see which parameters are most influential.

The next ten cases, 5 to 14, may be regarded as perturbations about Case 3, in which all the middle distributions were used. Cases 5 to 9 change one distribution from middle to low at a time, and Cases 10 to 14 change one from middle to high.

Cases 5 to 9 show that any low distribution suppresses bolt failure if combined with the other middle distributions. The changes have markedly different effects on bottom failure (2126 in Case 3). Pour diameter has the greatest effect, giving zero failures, followed by pour length and conversion ratio (4 and 5, insignificantly different) and then fraction of core molten with 172. Finally, changing the distribution of slug condensed phase fraction has no significant effect (2087 failures). These results are easily understood because bottom failure only depends on the explosion energy which is proportional to pour diameter squared, the pour length and the conversion ratio. It is unaffected by slug composition and is affected by core fraction molten only to the extent that this imposes a cutoff on the melt mass calculated from the pour geometry. Table I shows that changing to the low distribution of core molten changes the range of melt mass in the explosion from 7000 - 56000 kg to 0 - 31000 kg whereas changing to the low distribution of pour length restricts the melt in the explosion to 0 - 7000 kg.

Cases 10 to 14 perturb from Case 3 in the direction of greater damage. The ordering of importance, measured by the change from the base case value in Case 3, for bottom failure, is similar to that from Cases 5 to 9. Pour diameter has the greatest effect followed by pour length and conversion ratio close together; and fraction of core molten and slug composition have no significant effect. Fraction of core molten is now less important because it only makes a small change in cutoffs imposed on the mass in the explosion (see Table I).

The relative importance of these changes for vessel top failure is different however. The largest changes are now caused by changing the conversion ratio distribution, followed by pour diameter, followed by slug condensed phase fraction and pour length. Changing the distribution of fraction of core molten had no significant effect. This provides an illustration of the fact that the importance ranking of uncertainties can depend on the particular quantity that is of interest.

Cases 15 to 19 are perturbations from Case 4 in which all the high distributions were combined yielding nearly 100% failures in all categories. One low distribution at a time is now used. For vessel bottom failure the largest change is caused by changing the pour diameters, then fraction of core molten and conversion ratio (insignificantly different), then pour length. Slug composition caused no change. These changes can all be understood by considering the explosion energy. For bolt failure and missile velocities above 50 m/s changing the pour diameters still produces

the largest changes, followed now by conversion ratio, pour length and fraction of core molten, with slug composition still producing the smallest change. For missile velocities above 90 m/s, the changes in pour diameter, conversion ratio and fraction of core molten completely suppress missile formation, with pour length yielding the next largest change from Case 4 and slug composition still yielding the smallest change.

Cases 20 to 24 perturb from Case 2 in which all the low distributions were combined, leading to no failures of any kind. These cases show that this result is unchanged by using any one high distribution.

Summarizing the main calculations, the relative importance of the various parameters was found to depend on which particular kind of failure was investigated, and on which base set of distributions was perturbed. Generally the parameters directly defining the explosion energy, pour length and diameter and conversion ratio, were most important. Often the pour diameter had the largest influence, because it enters squared into the expression for explosion energy. The fraction of core molten often turned out not to be important because with the modeling and distributions used it acts as a cutoff on the mass of melt in an explosion; and in many of the cases sampled was either not effective or not the dominant restriction on the mass of melt in the explosion. To some extent this effect is an artifact of the way this model is parameterized. The slug condensed phase fraction does not affect vessel bottom failure; it sometimes significantly affected top failure but always ranked low among the five parameters investigated.

4.3 Results of Additional Calculations

In these calculations, values of the second set parameters were varied one at a time within their uncertainty ranges and combined with each of all the low, middle and high distributions of the first set parameters. Thus the effect of these changes over the whole range of the first set parameters is explored. Comparison with Cases 2, 3 and 4 allows the importance of changes in the second set parameters to be compared. Additionally, the effect of changing the upper limit of three first set parameters, fraction of core molten, conversion ratio and pour diameter, was investigated. These calculations are set out in Table V.

ABLE V. Additional Calculations

	Case	INPUT: Compare with Case Number	INPUT: Fraction Molten (%)	INPUT: Pour Diameter (m)	INPUT: Pour Length (m)	INPUT: Slug* Condensed Phase Fraction	INPUT: Conversion Ratio (%)	CALCULATIONS: Mean Explosion Energy (MJ)	CALCULATIONS: Mean Slug* Impact Energy (MJ)	CALCULATIONS: Mean Slug* Volume (m^3)	CALCULATIONS: Mean Slug* Mass (1000 kg)	FAILURES (per 10,000 trials): Vessel Bottom	FAILURES (per 10,000 trials): Bolts	FAILURES (per 10,000 trials): Large Missile V>50 m/s	FAILURES (per 10,000 trials): Large Missile V>90 m/s
Heat Content = 0.8 MJ/kg	25	2	L	L	L	L	L	7	1	9.3	16.9	0	0	0	0
	26	3	M	M	M	M	M	484	258	45.3	67.7	220	0	0	0
	27	4	H	H	H	H	H	2259	1320	22.6	53.8	10000	9394	9394	5799
Heat Content = 1.6 MJ/kg	28	2	L	L	L	L	L	15	2	9.3	16.9	0	0	0	0
	29	3	M	M	M	M	M	965	498	35.1	56.1	4118	89	89	10
	30	4	H	H	H	H	H	5109	2865	22.6	53.8	10000	10000	10000	10000
All Unmixed Melt and Water Above	31	2	L	L	L	L	L	11	1	9.3	16.8	0	0	0	0
	32	3	M	M	M	M	M	106	24	16.6	50.3	2094	1	1	0
	33	4	H	H	H	H	H	3826	2086	22.6	55.8	10000	9993	9993	9966
All Unmixed Melt and Water Below	34	2	L	L	L	L	L	11	1	9.2	16.7	0	0	0	0
	35	3	M	M	M	M	M	732	424	39.9	59.8	2099	2	2	0
	36	4	H	H	H	H	H	3830	2123	22.4	52.4	10000	10000	10000	9999
Variation of Fraction Molten	37	20	75-100	L	L	L	L	112	1	46.8	111.0	0	0	0	0
	38	10	75-100	M	M	M	M	749	344	54.6	124.0	2252	0	0	0
	39	4	75-100	H	H	H	H	4888	2518	26.0	74.4	10000	9753	9753	9677
Variation of Conversion Ratio	40	2	L	L	L	L	0-5.3	36	5	9.3	16.9	0	0	0	0
	41	3	M	M	M	M	5.3-10.7	2325	1136	26.2	46.4	9284	4304	4304	3053
	42	4	H	H	H	H	10.7-16.0	12292	7211	22.7	53.8	10000	10000	10000	10000
Lower Plenum Failure 500 MJ	43	2	L	L	L	L	L	11	1	9.3	16.9	0	0	0	0
	44	3	M	M	M	M	M	729	243	29.3	49.6	7101	0	0	0
	45	4	H	H	H	H	H	3838	2094	22.6	53.8	10000	9996	9996	9962
Lower Plenum Failure 1500 MJ	46	2	L	L	L	L	L	11	1	9.3	16.9	0	0	0	0
	47	3	M	M	M	M	M	733	490	45.3	67.7	254	0	0	0
	48	4	H	H	H	H	H	3821	2084	22.6	53.8	10000	9994	9994	9953
Small Pour	49	16	H	0.0-0.075	H	H	H	1.3	0.1	12.9	78.2	0	0	0	0

Cases 25 to 30 explore variation of the melt heat content. This enters into the equations modeling the explosion on exactly the same footing as the conversion ratio, that is, only in a product of terms defining the explosion energy. Thus it is expected to be rather important. Case 26 shows a drop from 2126 in Case 3 to 220 vessel bottom failures caused by reducing the heat content from 1.2 to 0.8 MJ/kg. In Case 27 the 10000 vessel bottom failures are unchanged, the 9987 missiles with v > 50 m/s only fall to 9394 but the 9959 missiles with v > 90 m/s fall to 5799. In the presence of the threshold effects in this problem, the effect of relatively small changes such as this may or may not affect a result depending upon whether they cause a large number of trials to move from one side of the threshold to the other.

Increasing the heat content to 1.6 MJ/kg, Cases 28 to 30, increased the bottom failures to 4118 (from 2126) and produced 89 bolt failures with missile velocity > 50 m/s instead of 1 in Case 3. Ten of these had missile velocities over 90 m/s (zero in Case 3). The increase in heat content was enough to produce 10000 missiles over 90 m/s in Case 30 compared with 9959 in Case 4. The isomorphism of the problem to conversion ratio and heat content means that the calculated results can be used to make further predictions; for example, results similar to Case 29 would be expected if a heat content of 1.2 MJ/kg were combined with a flat distribution of conversion ratio in the range 2.2 to 4.4%.

Cases 31 to 36 examine the effect of changing the assumption that the water that does not participate in an explosion lies below the explosion, and any unmixed melt lies above. In Cases 31 to 33 all the unmixed melt and water is located above the explosion, and in Cases 34 to 36 it is all below. Neither change alters the results of Cases 2, 3 and 4 significantly. This is because for explosions large enough to cause bolt failure there is little or no unmixed water; for the middle distributions, explosions strong enough to cause bolt failure will involve almost all the melt; and for the large distributions, again most of the melt is mixed. This insensitivity to the partition of material between the upward and downward moving slug means that the results are also insensitive to the assumed mass of water participating in the explosion. In the model used here, this water mass only affects the up/down partitioning.

Cases 37 to 39 explore the effects of fractions of core molten higher than 75%. Cases 37 and 38 which use a flat distribution from 75 to 100% show no significant difference from Cases 20 and 10 in which the range is 50 to 75%. Case 39 shows a very small reduction in bolt failure compared with Case 4 probably caused by increased tamping by unmixed melt over the explosion leading to lower slug velocities.

Cases 40 to 42 examine the effect of increasing the conversion ratio upper limit from 5 to 16%. These three cases use the same distributions as Cases 2, 3 and 4 except that the low, middle and high thirds of the range 0-16% are used for the conversion ratio. Case 40 shows that conversion ratios up to 5.3% are not sufficient to overcome the combined effect of the other small distributions. This is consistent with Case 24. Case 41 shows that a substantial number of failures of all kinds - 9284 vessel bottom and 3053 bolt failures with missile velocity greater than 90 m/s - are produced by combining all the middle distributions with conversion ratios from 5.3 to 10.7%. These are the highest numbers obtained in this study from any single change from Case 3 (all middle distributions). Case 42 using all large distributions and conversion ratios from 10.7 to 16.0% gives, as would be expected, 10000 failures in each category.

Cases 43 to 48 examine the effect of using different values for the energy required to fail the vessel bottom. As would be expected, this affects the number of vessel bottom failures where this is not 0 or 100%; Case 44 with a 500 MJ threshold gives 7101 failures, compared with Case 3 using 1000 MJ giving 2126 and Case 47 using 1500 MJ yielding 250 failures. The lack of any effect on the numbers of bolt failures is presumably because explosion energies up to 1500 MJ would not cause bolt failure even without vessel bottom failure.

Case 49 explores the effect of restricting the pour diameter to the size of one of the holes in the lower core plate. The maximum melt mass implied is 93 kg which by a wide margin is insufficient to damage the vessel. This mass is also similar to the limit proposed by Henry and Fauske [7, 25]. No failures were predicted.

To summarize the results of the additional calculations, varying the position of unmixed melt and water, varying the maximum fraction of core molten and varying the vessel bottom failure threshold did not significantly affect bolt failure or missile formation; varying the melt heat content had significant effects; and varying the maximum conversion ratio had a substantial effect.

5. Other Areas of Uncertainty

5.1 The Effects of High Pressure

The calculations and models described above all refer to steam explosions at ambient pressures at or near atmospheric. However, many important PWR accident sequences involve pressures up to about 17 MPa, the set point of the primary system safety valves. For example, in the Zion Probabilistic Safety Study the frequency of core melt following a large break loss of coolant accident is calculated to be 1.15×10^{-5} per year [45]. These are the sequences in which the pressure in the RPV is expected to be near to atmospheric. The total calculated core melt frequency for Zion is 4.21×10^{-5} per year [45]. Thus, the low pressure sequences are calculated to be 27% of all core melts for Zion. This percentage is uncertain and plant-specific.

The experimental data on steam explosions at elevated pressures are very sparse and inconclusive. Single droplet experiments indicate that, for constant water temperature, the triggering of explosions becomes easier for pressures above 0.1 MPa until about 0.8 MPa [33, 38, 46]. At 1.0 MPa, explosion triggering is comparable again to the 0.1 MPa case. At 1.1 MPa (the limit of the apparatus), triggering becomes slightly more difficult than at 0.1 MPa. At intermediate scale, 5.4 kg delivered to the water at an ambient pressure of 1.09 MPa did not explode spontaneously [17]. An explosion was, however, triggered with a detonator. Experiments have been conducted at Ispra which resulted in externally-triggered explosions under ambient conditions as high as 3.0 MPa [47]. Based on these and other data and models, it has been assumed that spontaneous triggering of steam explosions becomes less likely as the pressure increases, although explosions can still be induced by sufficiently large external triggers. While some external triggers, falling objects for example, may be found during reactor accidents, it is not known what trigger strength is required as a function of ambient pressure, nor what triggers will be available with what frequency.

Although the extrapolation of smalland intermediate-scale data at relatively low ambient pressures to large-scale events at much higher pressures seems plausible, it could conceivably be quite wrong. Single-droplet experiments show that explosion triggering becomes more difficult if noncondensable gases are present (hydrogen, oxygen, air) in the film around the droplet, or if the water subcooling is low. Intermediate-scale tests indicate that these suppressive mechanisms are not operative when the volume of the melt delivered is above a certain threshold [18]. It is not inconceivable that the suppressive effects of high ambient pressure might also be overcome at larger scales. There are simply no reliable data in this regime.

The following summarizes the effects that must be considered in any study accounting for high ambient pressure:

1. Trigger strength required as a function of pressure and scale.

2. At higher pressures, the volume production rate of steam in a coarse premixture will be lower than at low pressure, so that any limitation on mixing caused by steam generation may be weaker.

3. Small-scale results indicate that conversion ratio increases with ambient pressure [26, 38]. This may also be true at larger scale.

4. If the primary system is under pressure, the additional pressure increment to reach the failure threshold will be lower.

5. If lower plenum failure occurs, additional blowdown forces may contribute to the vessel's subsequent motion. [5]

6. Variation of material properties of water as a function of pressure.

Item 1 above would have the effect of reducing the calculated probabilities, possibly to zero, because of the possible improbability or impossibility of triggering steam explosions at high pressure. Items 2 through 5, on the other hand, have the potential to increase the calculated probabilities of failure. Thus the effects of uncertainties in steam explosion behavior and effects at high pressure may be either to increase or decrease the probabilities of vessel and containment failure calculated in Section 4. This is similar to the position adopted in Squarer's probabilistic analysis; he did not assign a probability for suppression of steam explosions at high pressure [12].

5.2 Uncertainty in Head Becoming a Missile

In this calculation, we have assumed containment failure due to impact by the vessel head. This failure mode requires that the head become a missile with a > 50 m/s velocity.

If the head is to become a missile, failure must occur at the bolts rather than at the top of the vessel top head. As discussed in Appendix B, it is uncertain whether the actual failure location is at the bolts or the top head. A second necessary condition is efficient coupling of the slug energy to the head. This requires that all the studs fail at approximately the same time. If this does not happen, the head may "can open" and the slug will continue, leaving the head behind.

If failure at the top of the vessel top head occurs before, or instead of, bolt failure, it is very uncertain what effect this would have on the failure probabilities calculated in Section 4. If the threshold for top head failure is lower than that for bolt failure, top head failure would generally have higher probabilities than those indicated for bolt failure. If there is to be any possibility of direct containment failure, a missile is required. This could either be a fragment of the top head, or the slug. Fragmentation of the top head, as distinct from the formation of flaps (open can-lid), might occur because of the substantial nonuniformity of the top head. The size and speed of any such fragments would be difficult to estimate. This would make their penetrating capability very uncertain. A similar situation could occur if, instead of the studs failing at approximately the same time, the studs fail in a zipping pattern. If this happens, the head could be spinning as it flies upward. In this situation, it is uncertain how much of the slug energy would be transferred to the head and what would be the consequence of a spinning head that may fly sideways to impact containment. The potential for the slug itself to be a damaging missile would appear to depend on whether it remains coherent or spreads out. This depends on details of the failure, and the slug flow pattern and so also is very uncertain.

The uncertainties in large missile formation that are due to uncertainty in the details of the failure processes at the top of the vessel may thus be bounded by two possibilities. On the one hand, formation of a large missile with penetrating power sufficient to breach containment may occur according to the criteria in Subsections 3.14 and 3.15. On the other hand the alternative mechanisms discussed in this Subsection and in Appendix B may always prevent the formation of missiles capable of damage.

5.3 Multidimensional and Geometric Effects

The modeling described in Sections 3 and 4 of this report only accounted for the gross geometrical features of the reactor pressure vessel and its internals. In particular, mixing of melt flowing from the core into the lower plenum with residual water there was assumed to be unimpeded except for the uncertain influence of steam production. Also the model of slug formation and propagation was one-dimensional. Geometrical features of the vessel can be identified which might affect the correctness of these assumptions and which contribute uncertainty. These are discussed in this subsection.

Almost all steam explosion experiments to date have been conducted in relatively uncluttered vessels. The lower plenum region of a PWR is relatively cluttered compared with these experiments. (The bottom of a BWR vessel is much more cluttered than a PWR.) This clutter may tend to inhibit the coarse mixing process prior to an explosion, by restricting lateral mixing [33]. The

increased surface area might also tend to trigger a number of (smaller) steam explosions, rather than a single large one. These possibilities have not yet been investigated experimentally. It is also conceivable that the presence of clutter (control rod tubes, instrumentation tubes, grates, etc.) could enhance mixing, and increase the amount of mass mixed and the ultimate explosion energy. The diffuser plate in a PWR might increase the degree of mixing of any melt passing through it. Furthermore, turbulent wakes and vortices might develop as the melt passes over and by various surfaces. This turbulence could increase mixing. In premixed gas phase combustion, obstacles and clutter can greatly increase the burning rate because the turbulence generated by those structures enhances mixing in front of a flame [26, 33]. Because the effects of lower plenum clutter are not known, they were not modeled in this study.

The actual vessel geometry is much more complex than the simple one-dimensional approximations employed in this study. Under some conditions, an explosion in the vessel lower plenum could vent up the downcomer annulus as well as up the core barrel. It is possible that such venting would ameliorate the forces on the upper head, but a detailed multidimensional calculation would be required to quantify this effect. Two-dimensional calculations have been performed with both the SIMMER [3] and CSQ [33] codes.

The SIMMER calculations identified important effects in the downcomer; water speeds of ~200 m/s were associated with explosions of peak energy ~1000 MJ and water slug impact peak pressures at the top of the downcomer were 30-100% of those calculated at the top head.

In the CSQ calculations "a small portion of the water slug" was forced up the downcomer [33]. Any difference between these results and those in the ZIP study is probably caused by different assumed boundary conditions. Further calculations of this kind would be needed to investigate the implications of downcomer flow more fully.

It is thus clear that multidimensional and geometric effects have the potential for both aggravating and mitigating the consequences of in-vessel steam explosions. Their neglect is thus a potential cause of underestimation of uncertainty, although in this study it is not important because of the wide range already identified.

5.4 The Effect of Correlations

The sampling from distributions described in Section 4 assumed that all the sampled parameters were independent; that is to say that knowledge of one of them does not change our knowledge of any other. If this assumption is wrong the affected parameters would be correlated. Our state of knowledge about these parameters is consistent with either the presence or the absence of correlations.

The qualitative effect of some potential correlations may be discussed by simple arguments. For example, it is possible that the heat content of the melt is correlated with fraction of core molten because a larger core melt may take longer to accumulate and hence may also accumulate more decay heat per unit mass. In comparison with Case 3 in Table IV, in which the melt heat content was constant, the range of possible explosion energies would be widened if heat content and fraction molten were correlated in this way. This is because masses of melt in explosions that were limited by small fractions of core molten would be combined with small melt heat contents; and explosions involving the largest melt masses permitted in Case 3 would have high melt heat contents. This effect on the tails of the explosion energy distribution would be particularly significant for the very low probability failures, increasing their probabilities to values intermediate between those of Cases 3 and 32 (in which the highest value of the heat content was used throughout).

The effects of potential correlations between parameters would be either to increase or to decrease the probabilities calculated in Section 4. Thus omitting potential correlations from our numerical calculations caused a potential understatement of the overall uncertainty in the probabilities.

5.5 Effects of Model Parameterization

The numerical results of the calculations described in Section 4 might be used to draw the following conclusions: that the probabilities of vessel failure and containment failure are uncertain over the range from 0 to 1; that estimates of these probabilities obtained from "middle" assumptions (Case 3) are about 21% and 10^{-4} respectively; and that the most important contributing uncertainties are those in the pour diameter and conversion ratio. These potential conclusions may depend on the arbitrary choices made of model parameterization and distributions. It is therefore necessary to consider whether the same conclusions would have been obtained, had different parameterizations or distributions been chosen.

First we consider the uncertainty ranges for the failure probabilities. Obviously a different parameterization, or a different set of combinations of distributions, could produce different ranges. For example, if all input distributions extended to the lower end of the parameter uncertainty ranges, having different upper limits, every combination of such distributions would include explosions of low energy which would cause no damage. Hence, all calculated damage probabilities would be less than one. This was illustrated in some preliminary calculations for this study published in reference 48. In those calculations lower limits of zero were used in all distributions for some parameters. Additionally the conversion ratio distributions were triangular (as in reference 11). Failure probability ranges of 0 to 51% for

the vessel and 0 to 33% for the containment were calculated. However if such a set of calculations were the only ones available it would be necessary to consider whether the full range of probabilities had been obtained. The ranges of probabilities set out in the present paper show that any narrower range would not include the full range of possibilities.

Second, we consider whether the "middle" probabilities obtained in Case 3 would be expected to change if different distributions or parameterizations were used. It is clear that they could change substantially in either direction. In comparison with the values in this paper (21% for the vessel and 0 to 10^{-4} for containment), the corresponding preliminary calculations in reference 48 yielded 1.5% for the vessel and 0 for containment, from a different "middle" set of distributions. Additionally, a different parameterization of the problem has been suggested [49] in which the area of the melt pour out from the core is used instead of its diameter. If the area parameterization is used, the middle third of the range of pour areas is 3.0 to 6.0 m^2, and if this is combined with the other middle distributions used in this report a mass range of 21,000 to 63,000 kg is obtained. This should be compared with the middle mass range of 7000 to 56,000 kg in Table I. The main effect of this parameterization change would therefore be to eliminate smaller melt masses (from 7000 to 21,000 kg) from the combination of middle distributons. The result would be intermediate between Case 11 (mass range 28,000 to 63,000 kg) and Case 12 (14,000 to 63,000 kg) in Table IV, and so calculated failure probabilities between 53 and 83% for the vessel and 0 and 1.8% for containment would be expected. Thus changes in distributions or parameterizations can substantially change the probabilities calculated from a "middle" combination, in either direction. Such probabilities must therefore be considered essentially arbitrary.

Finally, we consider whether the uncertainties in pour diameter and conversion ratio would continue to have the highest importance under a different choice of parameterization or distributions. Here, two points need to be made. First, under some different parameterizations the particular parameters discussed here might not be used; for example pour diameter is not explicitly included if the area representation described in the previous paragraph is used. In that case, the corresponding area parameter would assume high importance. More generally, the mass of melt participating in the explosion is important, because together with the conversion ratio it strongly affects the total explosion energy. The second point about relative importance of

parameter uncertainties is that such importance, if measured by the probability changes caused by changes of the parameters from one base case, will in general depend on the choice of the base case. The present calculations may be described as variations about three base cases (Cases 2, 3 and 4) that are rather widely distributed over the whole parameter space. Additionally, the important parameters found in these calculations are the same as those found in the preliminary calculations [48]. However, it is possible that in some unexplored part of the overall parameter space other parameters (like slug void fraction, or melt heat content) may assume high importance. It is therefore necessary to qualify the important uncertainties identified in the current calculations by noting that other uncertainties might be shown to be also important in parts of the parameter space not examined.

6. Discussion

The calculations in this report refer to in-vessel steam explosions at ambient pressures near to atmospheric. Numerical values were taken from the Zion reactors. They show that the conditional probability of containment failure, given core melt during a low-pressure accident, is extremely uncertain. Indeed the results span the range of probability from 0 to 1. This uncertainty estimate is derived from the particular choice of distributions and combinations thereof used. Adequate evidence does not exist at present to exclude any of these combinations, or the probabilities calculated from them, and such evidence would be required in order to establish a narrower range of probability. If all the "middle" distributions in this study are combined, a value of ~ 10^{-4} is obtained. This however should not be used as a best estimate of the fraction of core melt accidents leading to containment failure by steam explosions, because a different parameterization of the problem could give a completely different number and because it is derived from single assignments of subjective probabilities. The effect of alternative assignments needs to be considered, and this leads to the range of results calculated here.

Examination of Tables IV and V shows that the criterion of an explosion energy > 1000 MJ for vessel failure at the base led to a significant probability of such failure for many of the cases sampled. The uncertainty in this probability also covers the range from 0 to 1. The possibility of explosive vessel failure should be taken into account when planning action in response to core-melt accidents that still have the potential for recovery to a coolable state in-vessel.

Extension of these results to higher pressures would in principle require reformulation of the problem to account for the different characteristics of triggering and possibly mixing. However in practice the range of uncertainty can be explored by qualitative arguments: on the one hand steam explosions may be impossible in reactors above some value of the pressure, in which case the probability of containment failure by this mode would be zero. On the other hand effective external triggering may be probable, in which case the current calculations would have to be modified to take account of the effects listed in subsection 5.1. Some of these effects, namely possibly easier mixing, possible conversion ratio increases, increased ease of vessel failure, and blowdown forces from vessel failure at pressure, have the potential to increase failure probabilities. Thus extension to higher pressures introduces effects that may reduce, and others that may increase failure probabilities. The uncertainty intervals estimated for the probabilities would therefore be unchanged.

Extension of the results to other plants may in some cases in practice be possible by rather simple comparisons of dimensions to determine whether any significant differences exist, and if so, whether they are large enough to affect the results of the current calculations materially.

The extensive sensitivity study presented here shows that the uncertainties in two parameters out of the ones used in the model are highly important: pour diameter and conversion ratio. The prominence of the first of these is to some extent an artifact of the model, in that it appears squared in the expression for explosion energy (other parameters appearing linearly). A more general statement would be that the mass of melt participating in an explosion is highly important.

This mass is in turn determined by two highly uncertain processes: the process of core melting which may or may not produce and release a large pool of melt coherently; and the process of melt - water mixing which may or may not be effectively self-limiting due to steam production.

The conversion ratio is uncertain because it is not known whether this parameter decreases, remains within the bounds of current measurements or increases as the melt mass increases from kilograms to thousands of kilograms.

An additional factor influencing the probability of containment failure, that was not accounted for in the sensitivity study, is the question whether the interaction of a slug with the top of the vessel can produce damaging missiles or not. Since the uncertainty in the vessel failure modes that determine the answer to this question can reduce the containment failure probability to zero, this uncertainty is of high importance.

Thus four of the most important contributors to the uncertainty in the probability of containment failure due to steam explosions are the conversion ratio, the mass of melt participating in the explosion, the likelihood of triggering at high pressure and the failure mode of the vessel top head. Because this study is based on a finite sampling from a parameter space, other uncertainties may also be important. Substantial reduction of any of these important uncertainties would, if the result were favorable, substantially reduce the uncertainty in the probability of containment failure due to steam explosions. For a significant containment failure probability, either a significant probability of conversion ratios higher than currently measured or a significant probability of large masses of molten core actively participating in an explosion would be needed. Additionally, triggering in the pressure range of importance and large missile formation would have to be possible.

REFERENCES

1. N. C. Rasmussen (Ed.), Reactor Safety Study: An Assessment of Accident Risks in US Commercial Nuclear Power Plants, WASH-1400, NUREG 75/014, (Washington, D. C., October, 1975).

2. W. B. Murfin (Ed.), Report of the Zion/Indian Point Study - Vol. I, NUREG/CR-1410, SAND80-0617/1, (Albuquerque, NM, August, 1980).

3. M. G. Stevenson (Ed.), Report of the Zion/Indian Point Study: Volume 2, NUREG/CR-1411, LA-8306-MS, (Los Alamos, NM, April, 1980).

4. The German Risk Study Summary (Cologne, Germany: Gesellschaft fuer Reaktorsicherheit mbH, 1979).

5. J. H. Gittus (Ed.), PWR Degraded Core Analysis, NDR-610(S), (Springfields, UK, April, 1982).

6. Steam Explosions in Light Water Reactors, Report of the Swedish Government Committee on Steam Explosions, DsI 1981:3, (Stockholm, 1981).

7. R. E. Henry and H. K. Fauske, Required Initial Conditions for Energetic Steam Explosions, presented at ASME Winter Meeting, (Washington, D. C., November, 1981).

8. T. G. Theofanous and M. Saito, An Assessment of Class 9 (Core-Melt) Accidents for PWR Dry Containment Systems, Nucl. Eng. Des. 66, 301-332, (September, 1981).

9. Preliminary Assessment of Core Melt Accidents at the Zion and Indian Point Nuclear Power Plants and Strategies for Mitigating Their Effects, U. S. Nuclear Regulatory Commission, NUREG-0850, Vol. 1, (Washington, D. C., November, 1981).

10. F. Mayinger, Kernschmelzunfall: Wie sind Dampfexplosionen in Licht neuerer Erkentnisse zu beurteilen? Zu Moeglichkeit, Ablauf und Wirkung, Atomwirtschaft, pp. 74-81, (February, 1982), English translation: UKAEA Risley Trans 4636.

11. D. V. Swenson and M. L. Corradini, Monte Carlo Analysis of LWR Steam Explosions, NUREG/CR-2307, SAND81-1092, (Albuquerque, NM, October, 1981).

12. D. Squarer and M. C. Leverett, Steam Explosion in Perspective, Proc. Int. Meeting on LWR Severe Accident Evaluation, Cambridge, MA, August 1983, pp. 6.1-1 to 6.1-9.

13. T. A. Dullforce, The Spontaneous Triggering of Small Scale Vapour Explosions, Ph.D. Thesis, University of Aston in Birmingham, (October, 1981).

14. Commonwealth Edison Company, Zion Station Final Safety Analysis Report, Docket 50295-16 and 50304-16, (Chicago, IL, December, 1970).

15. L. D. Buxton and W. B. Benedick, Steam Explosion Efficiency Studies, NUREG/CR-0947, SAND79-1399, (Albuquerque, NM, November, 1979).

16. D. E. Mitchell and N. A. Evans, Intermediate Scale Steam Explosion Phenomena - FITSB Series, NUREG/CR-0000, SAND83-1057, (Albuquerque, NM, 1984, to be published).

17. D. E. Mitchell, M. L. Corradini and W. W. Tarbell, Intermediate Scale Steam Explosion Phenomena: Experiments and Analysis, NUREG/CR-2145, SAND81-0124, (Albuquerque, NM, September, 1981).

18. Memorandum from M. Berman and N. A. Evans to R. W. Wright, USNRC, Effects of Scale On Steam Explosions, March 31, 1983.

19. M. L. Corradini, Analysis of Molten Fuel-Coolant Interactions, Progress Report for the Period April to September 1982, UWRSR4 (Madison, WI, 1982).

20. M. Berman (ed), Light Water Reactor Safety Research Program Semiannual Report, April - September 1982, NUREG/CR-3407, SAND83-1576, (Albuquerque, NM, 1983).

21. M. J. Bird, Thermal Interactions Between Molten Uranium Dioxide and Water, An Experimental Study Using Thermite Generated Uranium Dioxide, Presented at ASME Winter Meeting, (Washington, D. C., November, 1981).

22. M. Berman and R. K. Cole, Status of Core Melt Programs - May-June 1983, Memo to T. J. Walker and S. B. Burson, USNRC (Albuquerque, NM, October 1983).

23. M. Berman and R. K. Cole, Status of Core Melt Programs - July-August 1983, Memo to T. J. Walker and S. B. Burson, USNRC (Albuquerque, NM, October 1983).

24. M. Berman (ed), Light Water Reactor Safety Research Program Semiannual Report, April-September 1983, (Albuquerque, NM, forthcoming).

25. H. K. Fauske, Scale Considerations and Vapor Explosions (Rapid Phase Transitions), Presented at LNG Safety Workshop, MIT, (March, 1982).

26. M. Berman (Ed.), Light Water Reactor Safety Research Program Semiannual Report, October, 1981 - March, 1982, NUREG/CR-2841, SAND82-1572, (Albuquerque, NM, December, 1982).

27. M. L. Corradini, A proposed model for Fuel-Coolant Mixing, Trans. ANS 41, 415-416, (1982).

28. M. L. Corradini, Proposed model for Fuel-Coolant Mixing during a Core-Melt Accident, Proceedings of the International Meeting on Thermal Nuclear Reactor Safety, Chicago, IL, August 1982, NUREG/CP-0027, Vol. 2, pp. 1399-1408.

29. M. L. Corradini and G. A. Moses, A Dynamic Model for Fuel-Coolant Mixing, Proc. Int. Meeting on LWR Severe Accident Evalution, Cambridge, MA, August 1983, pp. 6.3-1 to 6.3-8.

30. M. Berman and R. K. Cole, Status of Core Melt Programs - November-December 1983, Memo to J. L. Telford and S. B. Burson, USNRC (Albuquerque, NM, February 1984).

31. M. Berman (ed), Light Water Reactor Safety Research Program Semiannual Report, October 1983-April 1984 (Albuquerque, NM, forthcoming).

32. G. A. Greene et al, Some Observations on Simulated Molten Debris - Coolant Layer Dynamics, Proc. Int. Meeting on LWR Severe Accident Evalution, Cambridge, MA, August 1983, pp. 12.2-1 to 12.2-7.

33. M. Berman (Ed.), Light Water Reactor Safety Research Program Semiannual Report, April - September, 1981, NUREG/CR-2481, SAND82-0006, (Albuquerque, NM, February, 1982).

34. A. T. Chamberlain and F. M. Page, An Experimental Examination of the Henry-Fauske Voiding Hypothesis (University of Aston, Birmingham, UK, 1983).

35. R. Haag and H. Korber, Zusammenstellung wichtiger Ergebnisse und Ableitung von Kenntnislucken zum Problemkreis Kernschmelzen, BMFT-150-400 (Gechingen, Germany, 1980).

36. L. D. Buxton, W. B. Benedick and M. L. Corradini, Steam Explosion Efficiency Studies, Part II: Corium Experiments, NUREG/CR-1746, SAND80-1324, (Albuquerque, NM, October, 1980).

37. H. K. Fauske and R. E. Henry, Interpretation of Large Scale Vapor Explosion Experiments with Application to Light Water Reactor (LWR) Accidents, Proc. Int. Meeting on LWR Severe Accident Evalution, Cambridge, MA, August 1983, pp. 6.5-1 to 6.5-5.

38. L. S. Nelson and P. M. Duda, Steam Explosion Experiments with Single Drops of Iron Oxide Melted with a CO_2 Laser, Part II, Parametric Studies, NUREG/CR-2718, SAND82-1105, (Albuquerque, NM, To be Published).

39. M. L. Corradini and D. V. Swenson, Probability of Containment Failure Due to Steam Explosions Following a Postulated Core Meltdown in an LWR, NUREG/CR-2214, SAND80-2132, (Albuquerque, NM, June, 1981).

40. K. McFarlane, Conservative (Hicks-Menzies) Results for the Efficiency and Work Capacity of an In-vessel Steam Explosion, NST/PWR9(81)17 (Culcheth, UK, 1981).

41. V. E. Denny and B. R. Sehgal, Analytical Prediction of Core Heatup/Liquefaction/Slumping, Proc. Int. Meeting on LWR Severe Accident Evaluation, Cambridge, MA, August 1983, pp. 5.4-1 to 5.4-9.

42. R. P. Kennedy "A Review of Procedures for the Analysis and Design of Concrete Structures to Resist Missile Impact Effects," Nuclear Engineering and Design, Vol. 37, pp. 183-203, (1976).

43. R. P. Kennedy "Local Missile Impact Effects," Extreme Load Post Conference Seminar, SMIRT 5, Engineering Decision Analysis Co., Inc. (1979).

44. C. Berriaud, A. Sokolovsky, R. Gueraud, T. Dulac and R. Labrot, "Local Behaviour of Reinforced Concrete Walls Under Hard Missile Impact," Paper J 7/9, 4th International Conference on Structural Mechanics in Reactor Technology, (SMIRT 4, 1977), Nuclear Engineering and Design 45, 457-469 (1978), English translation: SAND77-6021 (Albuquerque, NM, 1977).

45. Commonwealth Edison Co., Zion Probabilistic Safety Study, Chicago, 1981.

46. L. S. Nelson and P. M. Duda, Steam Explosions of Molten Iron Oxide Drops: easier initiation at small pressurizations, Nature 296, 844-846 (1982).

47. R. Hohmann, H. Kottowski, H. Schins and R. E. Henry, Experimental Investigations of Spontaneous and Triggered Vapour Explosions in the Molten Salt/Water System, Proceedings of the International Meeting on Thermal Nuclear Reactor Safety, Chicago, IL, August 1982, NUREG/CP-0027, Vol. 2, pp 962-971.

48. M. Berman, D. V. Swenson and A. J. Wickett, Trans ANS 45, 378-380 (1983).

49. J. B. Rivard, Personal Communication (1983).

APPENDIX A

SUBJECTIVE PROBABILITY

A subjective probability is a numerical expression of an individual's degree of partial belief in the truth of a proposition [A-1, A-2] In the current case, degrees of belief in propositions such as "the conversion ratio lies between 1.4% and 1.5%" are the basis of the probability distributions. Textbooks provide operational definitions of subjective probability similar to the following. "If an individual would offer betting odds for small bets of 1 to n that a proposition were true and n to 1 that it were false, then his subjective probability of its truth is 1/(1 + n)."

The following properties of subjective probabilities follow from the definition:

1) They comply with the usual laws for combining probabilities.

2) If sufficient data or evidence exist to justify a classical frequentist probability (fraction of successes out of a large number of trials) the subjective probability must be consistent with it.

3) If a frequentist probability statement cannot be justified, different individuals aware of the same evidence may quote different subjective probability values.

This last property, non-uniqueness, means in the circumstances of the current problem, that any subjective probability distributions of the uncertain parameters are uncertain and must, in an uncertainty study, themselves be varied within the ranges of uncertainty of the parameters that they describe.

REFERENCES

A-1 D. V. Lindley, Introduction to Probability and Statistics from a Bayesian Viewpoint (Cambridge University Press, UK, 1965).

A-2 D. H. Mellor, The Matter of Chance (Cambridge University Press, UK, 1971).

APPENDIX B

FINITE ELEMENT CALCULATION OF VESSEL FAILURE

Introduction:

In the main body of this report, a fracture criterion was used to evaluate failure of the bolts. To do this, the slug impact pressure load on the head was assumed to be transmitted to the bolts. The resulting stress was compared with the fracture strength of the bolts. In this Appendix, we justify this approach and provide additional background into failure of the reactor vessel due to an internal steam explosion. Similar calculations and a more detailed discussion are given in Ref. B-1.

The goal is to determine the sequence in which failures will occur and hence to provide a basis for choosing failure locations in the vessel. However, failure prediction under high strain dynamic conditions for as complicated a structure as the reactor vessel is very uncertain. We have approached this problem using a simplified finite element model of the reactor vessel. Calculated stresses and strains were then compared to either a strain or fracture failure criterion, as appropriate for different parts of the vessel.

Material Properties:

Typical material properties were used in the analysis to obtain estimates of vessel response. The vessel is constructed of A533 steel and the bolts are made of SA-540 steel. Values of the material properties were obtained from References B-2 and B-3 and are listed in Table B-1.

TABLE B-1

Table B-1: Material Properties at 288°C (Typical Values from References B-2 and B-3)

MATERIAL	YOUNG'S MODULUS (10^9Pa)	YIELD STRESS (10^6Pa)	ULTIMATE STRESS* (10^6Pa)	STRAIN* AT FAILURE	DENSITY (kg/m^3)	FRACTURE TOUGHNESS (10^6 N-m$^{-3/2}$)
VESSEL A-533	177	422	598	0.20	8000	275
BOLTS SA-540	177	892	1052	0.19	8000	175

*These are the Engineering stress and strain, that is, the force divided by the initial area and the deflection divided by the initial length. The logarithmic strain at failure, that is, the natural logarithm of the current length divided by the initial length, is 0.18 for the vessel.

Failure Criteria:

In this analysis, two failure criteria were used: strain failure and brittle fracture. Strain failure occurs if a material is excessively deformed until voids form and coalesce, leading to loss of strength. Brittle fracture occurs as a result of flaws in the structure. If the energy released due to crack growth is greater than the energy to extend the crack, brittle failure occurs. Based on previous calculations [B-1], the two locations of likely failure are the top of the head at the centerline and the bolts. The strain criterion was used at both locations, while the fracture criterion was used only at the bolts. (Brittle fracture of the head is not expected because the head material is more ductile than the bolts.)

Strain failure was evaluated by comparing the calculated effective plastic strain to the uniaxial failure strain. The effective plastic strain is defined by:

$$\bar{\varepsilon}_{p\ell} = \frac{\sqrt{2}}{3} \left[(\varepsilon_1 - \varepsilon_2)^2 + (\varepsilon_2 - \varepsilon_3)^2 + (\varepsilon_3 - \varepsilon_1)^2\right]^{1/2}$$

For uniaxial loading, the effective plastic strain is the equal to the uniaxial strain, but for biaxial loading conditions (as experienced in the vessel head), the use of effective plastic strain leads to failure at biaxial strains smaller than the uniaxial failure strain. This is consistent with experimental observation [B-4].

The second failure criterion was based on fracture mechanics calculations. (For a discussion, see a standard text such as Reference B-5.) For this analysis, the stress intensity factor was calculated using linear elastic fracture mechanics and a design flaw size recommended by the Pressure Vessel Research Committee [B-6]. This is a 7.6 mm deep circumferential crack for the bolts. As shown in Figure B-1, the stress intensity is a function of the bolt diameter, D, the unflawed diameter, d, and the applied load, p, (or alternately, axial stress in the bolt, σ) [B-7].

$$K_1 = \frac{\pi}{4} D^{1/2} \left[1.72 \left(\frac{D}{d}\right) - 1.27\right]\sigma$$

Substituting values appropriate for the bolt diameter, D = 0.1778 m, and the unflawed diameter assuming the design flaw, d = 0.1625 m, we obtain:

$$K_1 = 0.202\sigma \quad N\text{-}m^{-3/2}$$

Knowing the fracture toughness of the bolt material, K_{frac} = 175 $MN\text{-}m^{-3/2}$, we can solve for the stress in the bolts to give failure:

$$\sigma_{fracture} = \frac{K_{frac}}{0.202} = 870 \text{ MPa}$$

For the bolts, the fracture stress is below the yield stress. It can also be shown that the size of the plastic zone at the crack tip is small compared to the bolt diameter. Because plane strain linear elastic fracture mechanics assumptions are satisfied, the calculated fracture stress is a reasonable estimate of the true fracture stress. Therefore, it is expected that the studs would fail by brittle fracture if the assumed flaw was present. If smaller flaws were present (d > 0.165 m), the yield strength of the bolts is exceeded before the fracture stress is reached, and the bolts would likely fail by plastic deformation.

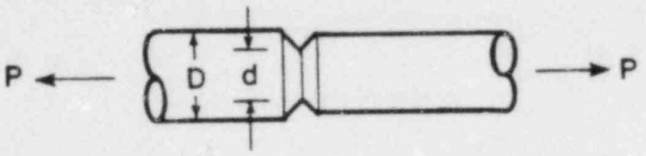

$$K_I = \frac{P}{D^{3/2}} \left[1.72\left(\frac{D}{d}\right) - 1.27\right]$$

$$K_I = \left(\frac{\pi}{4}\right)(D)^{1/2} \left[1.72\left(\frac{D}{d}\right) - 1.27\right]\sigma$$

Figure B-1: Bolt Stress Intensity Calculation [B-7]

Numerical Model:

A finite element model was used to evaluate the response of the closure head to impact by material accelerated from below. The structural model, which represents the reactor vessel above the nozzle center lines, is shown in Figure B-2. This model was developed using the HONDO II [B-8] computer code which can calculate the large deformation, dynamic response of axisymmetric solids. Because failure of the bolts could lead to a large mass missile (the top head), the bolts were modeled separately from the flanges. The bolt material properties were reduced to account for the difference in area between the solid ring in the axisymmetric model and the actual bolt area. Sliding interfaces were used between the flanges and between the top flange and the bolt nut to give a fairly accurate representation

of bolt/flange behavior during impact. Based on the Zion FSAR [B-9], the bolts were pretensioned to a stress of 290 MPa. The model did not include the effects of the penetrations at the top of the closure head. These penetrations would be expected to reduce the strength of the top of the head and to increase the possibility of head failure.

Loading Conditions:

As described in the main body of this report, we have modeled the slug impact as applying an approximately uniform pressure to the vessel head. This loading is similar to the loading calculated by the Los Alamos National Laboratory (LANL) using the SIMMER code [B-10]. Using the calculated bolt fracture stress, the bolt area, and the vessel dimensions, the static pressure in the head required to fracture the bolts is approximately 80 MPa.

Four finite element calculations were made near to the 80 MPa fracture pressure. These included ramp loadings of 60, 80, and 100 MPa, and a step loading of 80 MPa. For the ramp loading, the pressure was ramped to the peak value over 5 ms, held constant for 8 ms, and then ramped down to zero in 5 ms. The step loading was applied for a period of 13 ms. The purpose of the step loading was to examine the effect of dynamic overshoot, since a ramp of 5 ms is sufficiently long relative to the period of natural vibration of the head that it can be considered an essentially static loading. Because the slug will likely be somewhat diffuse by the time it loads the head, it seems reasonable to expect the loading to be closer to a ramp. Once again, we should note that these loading conditions are similar to those calculated by LANL using SIMMER [B-10].

Results:

Figure B-3 shows displacement plots for the 80 MPa ramped loading initially and after the pressure has been applied for 0.0013 sec. Figures B-4 through B-6 show plots of the results used to evaluate fracture for the 60 and 80 MPa ramp cases and the 80 MPa step case. A summary of all fracture evaluations is given in Table B-2.

For the 60 MPa ramp loading, only small plastic strains occur. The bolt stresses do not overshoot the static stresses significantly, confirming that the ramp loading is essentially static. No failure is predicted for this loading case.

Increasing the pressure to 80 MPa with a ramp loading causes significant plastic strain in the head as shown both in the displacement plots (Figure B-3) and head strain plot (Figure B-6).

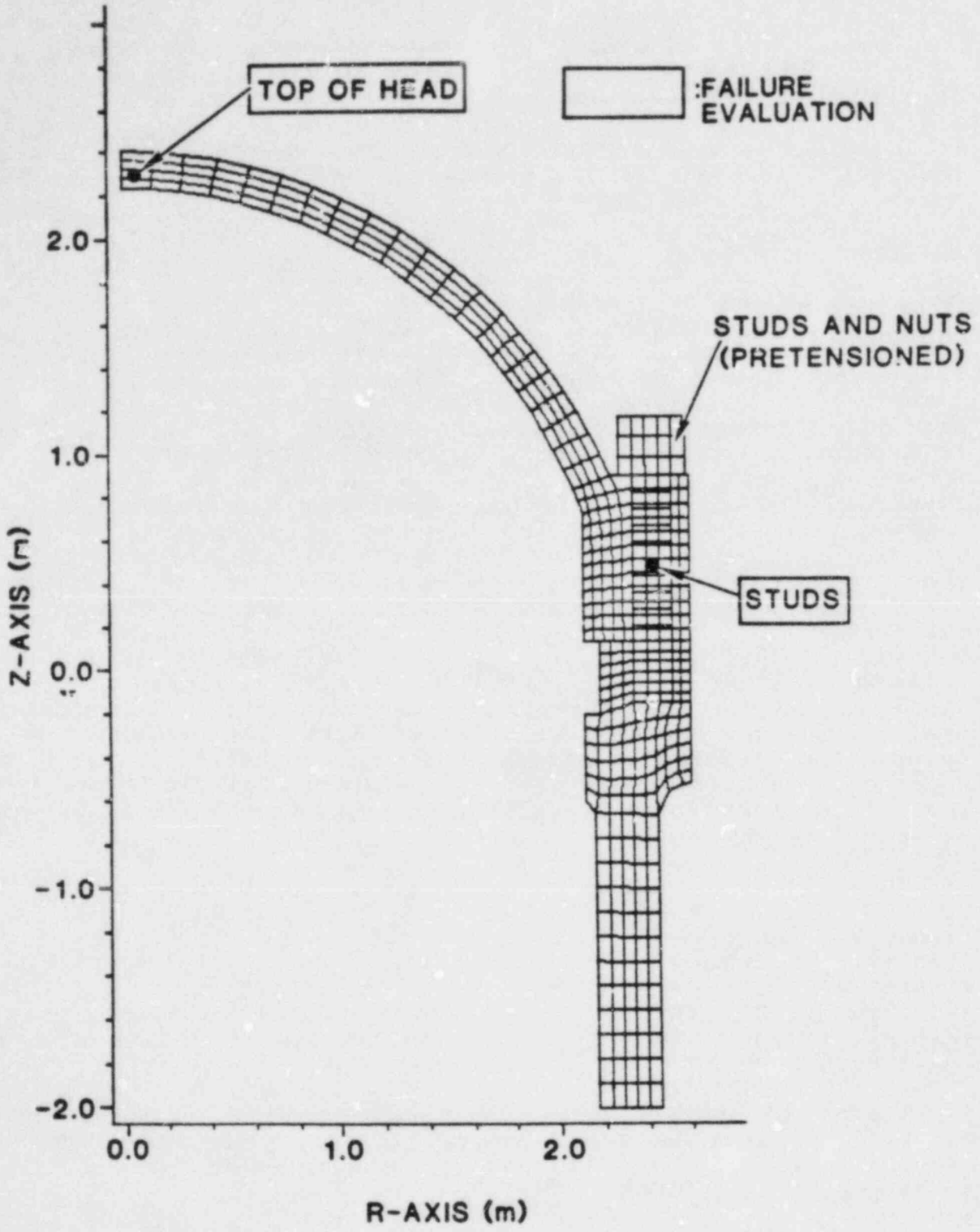

Figure B-2: Finite Element Model and Location of Failure Evaluation

Table B-2: Loading Cases Analyzed Using Finite Element Model and Failure Evaluation

CASE	Bolt Stress*		Stud Plastic Strain+		Head Plastic Strain+	
	Max (MPa)	t_{fail} (ms)	Max	t_{fail}	Max	t_{fail} (ms)
60 MPa Ramp	690	None	0.0	None	0.0001	None
80 MPa Ramp	950	9	0.0008	None	0.12	None
100 MPa Ramp	1350	4	0.085	None	0.38	9
80 MPa Step	1100	2	0.0075	None	0.16	None

* True stress

+ Logarithmic strain (see footnote to Table B-1)

However, failure is not predicted in the head. The stud stresses exceed the fracture stress (Figure B-4) and a relatively small amount of plastic strain occurs in the studs. Based on these results, it appears possible for fracture of the studs to occur without failure at the top of the head. Whether this will occur is not exactly clear since the penetrations in the head could weaken the top of the head. Previous calculations [B-1], predicted failure of the head rather than stud failure. The difference between these calculations is that a more spatially uniform loading of the head is assumed here, rather than loading which was biased towards the center of the head.

For the 100 MPa ramp loading (Table B-2), failure was predicted at both the studs and the head. The stud fracture criterion was attained before the head failure criterion.

Finally, the effect of step loading can be seen by comparing the 80 MPa step loading results to the 80 MPa ramp results. Step loading of the head causes higher stud stresses and greater plastic strain in the head. However, as for the 80 MPa ramp loading, only fracture of the studs is predicted for the 80 MPa step loading.

a. INITIAL CONFIGURATION

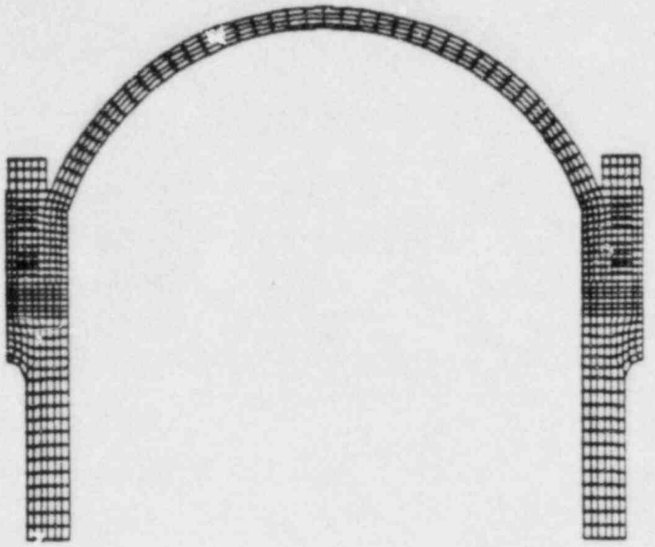

b. AFTER 0.013 sec LOADING

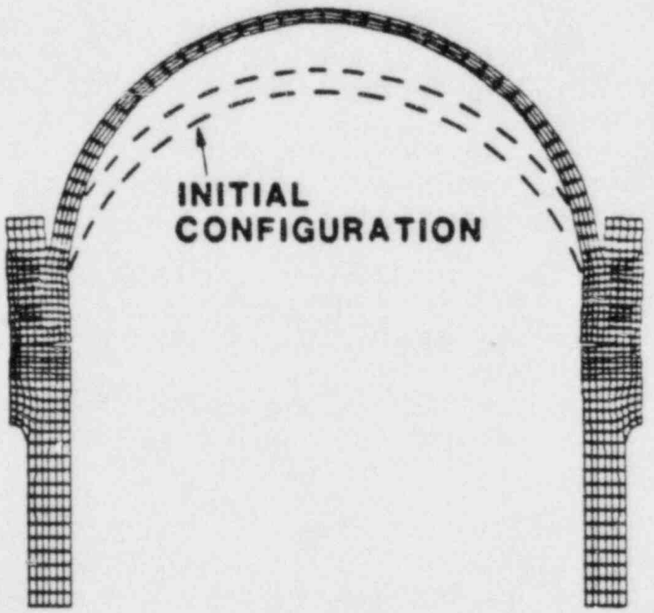

Figure B-3: Head Displacements for 80 MPa Ramp Loading
(Magnification = 2)

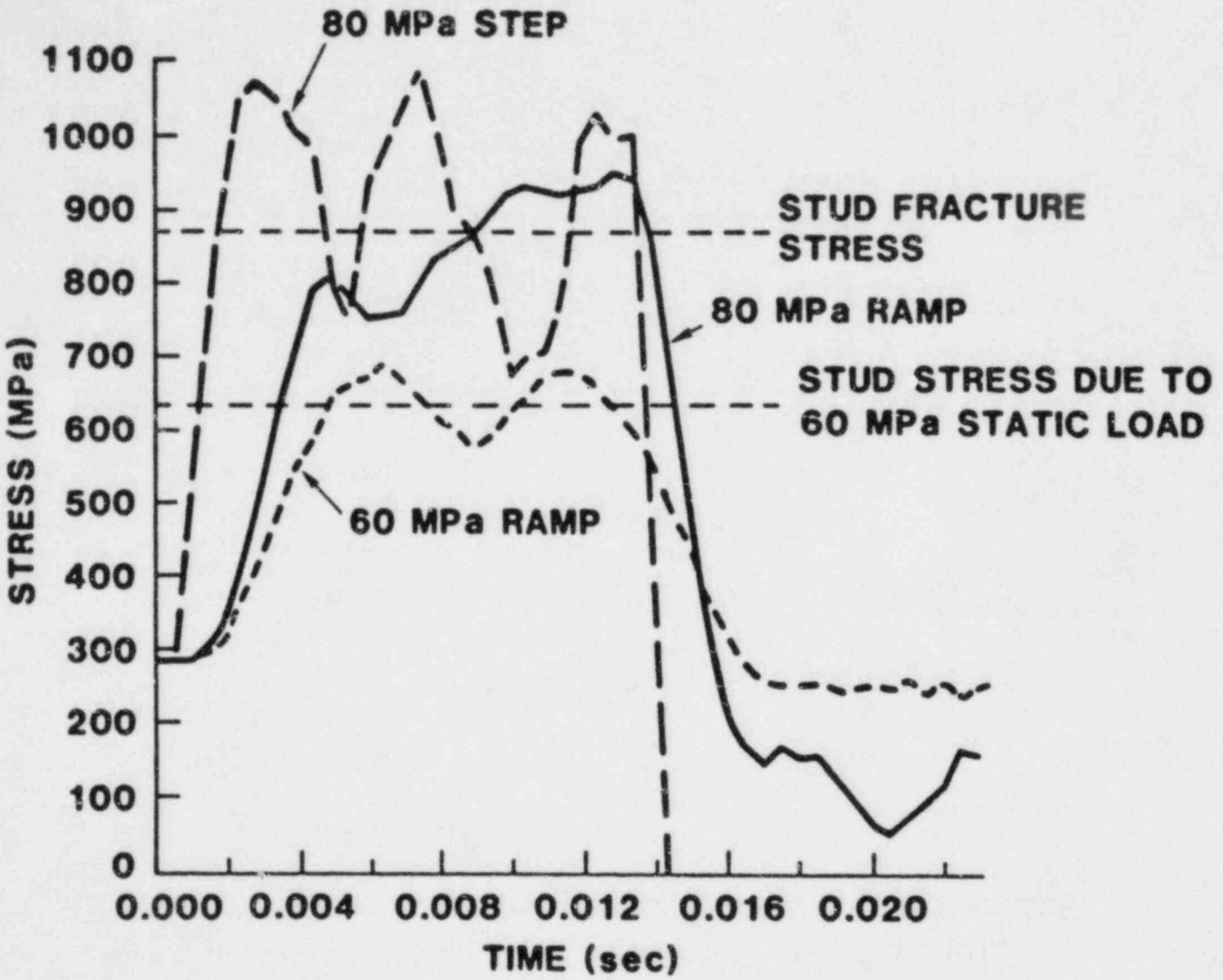

Figure B-4: Average Axial Stress in Studs

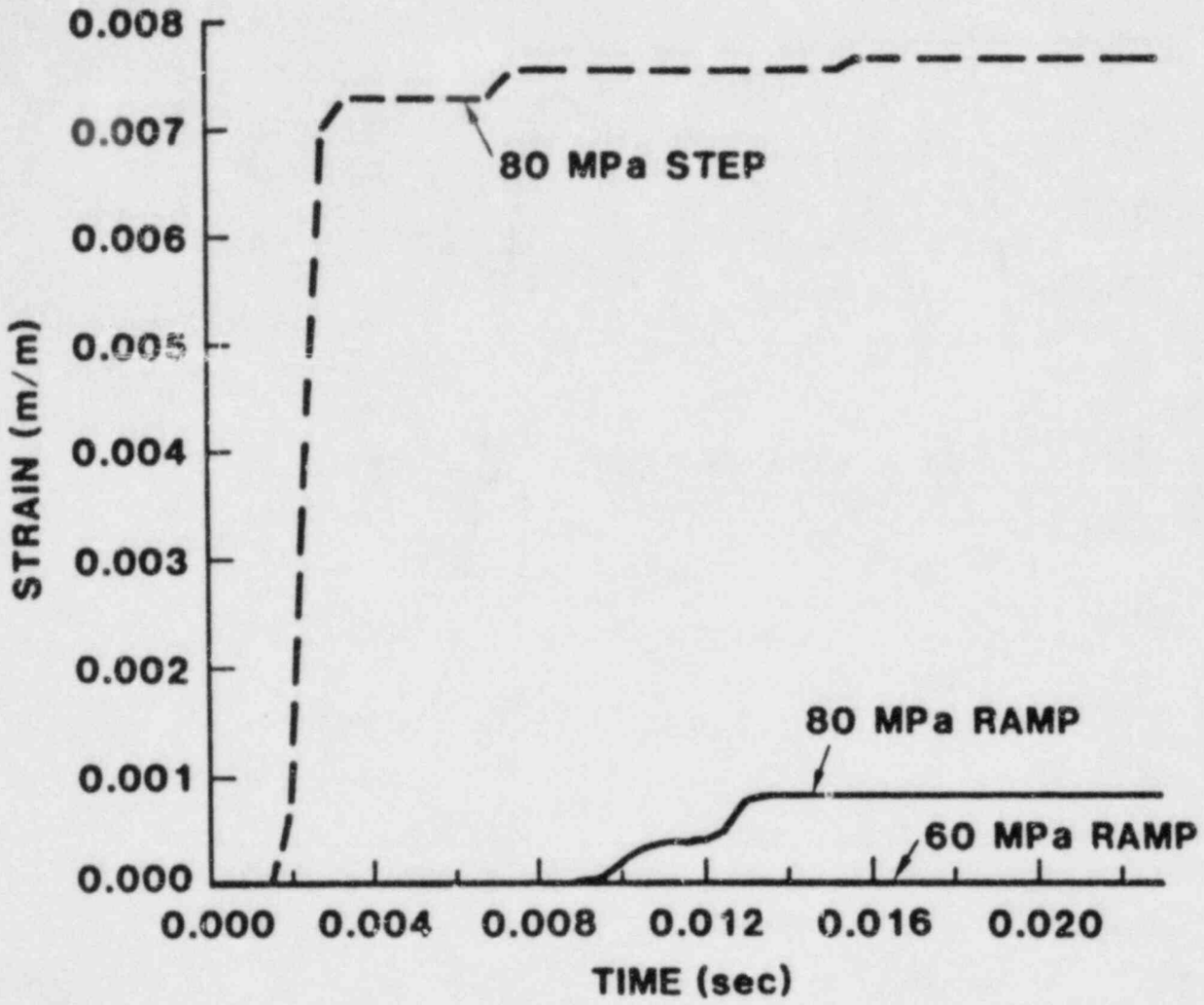

Figure B-5: Average Effective Plastic Strain in Studs

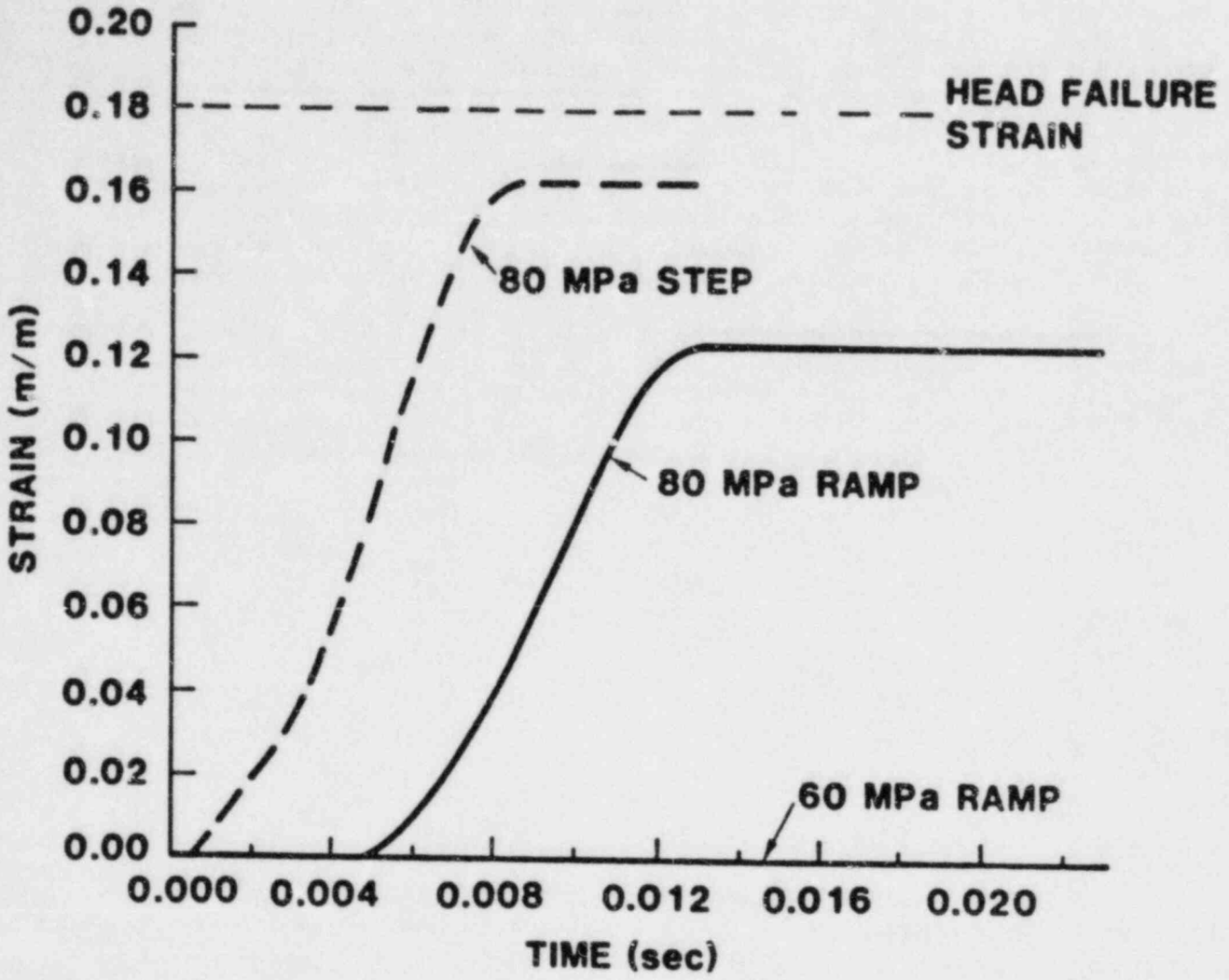

Figure B-6: Average Effective Plastic Strain at Center of Head

Summary:

The loading conditions we have examined are more spatially uniform than those arising from impact by a solid water slug [B-1] which tended to concentrate the loading to the center of the head. Instead, they approximate the LANL loading conditions predicted using SIMMER [B-8]. For this more spatially diffuse loading, the location of failure is uncertain. This should be expected, since the loading is similar to a static pressure loading for which the vessel is designed. Good design implies approximately equal strength for all failure modes. Because of the change in loading, bolt failure is more likely in this study than in reference B-1.

Assuming flaws exist in the bolts, bolt fracture is predicted to occur before head failure. Thus, it is plausible that the bolts could fail and the head become a missile. This is the assumption we have used in Sections 3 and 4 of this report. Subsection 5.2 discusses the effects of the alternative possibility of head failure before bolt failure.

REFERENCES

B-1 M. L. Corradini and D. V. Swenson, "Probability of Containment Failure Due to Steam Explosions Following a Postulated Core Meltdown in an LWR," NUREG/CR-2214, SAND80-2132, Sandia National Laboratories, (Albuquerque, NM, June, 1981).

B-2 Letter from R. R. Seeley (Babcock and Wilcox Research and Development Division) to D. V. Swenson, (February, 1980).

B-3 W. L. Server and W. Oldfield, "Nuclear Pressure Vessel Steel Data Base," EPRI NP-933, Electric Power Research Institute, Palo Alto, CA, Project 886-1, Topical Report, (December, 1978).

B-4 A. K. Ghosh, "A Criterion for Ductile Fracture in Sheets Under Biaxial Loading," Metallurgical Transactions, Vol. 7A, (April, 1976)

B-5 D. Broek, Elementary Engineering Fracture Mechanics (Martinus Nijhoff, The Hague, 1982.)

B-6 WRC Bulletin 175, "PVRC Recommendations on Toughness Requirements for Ferritic Materials," Pressure Vessel Research Committee, (August, 1972).

B-7 G. C. Sih, Handbook of Stress Intensity Factors, Institute of Fracture and Solid Mechanics, Lehigh University, (Bethlehem, PA, 1973).

B-8 S. W. Key, Z. E. Beisinger and R. D. Krieg "HONDO II, A Finite Element Computer Program for the Large Deformation Dynamic Response of Axisymmetric Solids," SAND78-0422, Sandia Laboratories, (Albuquerque, NM, October, 1978).

B-9 Commonwealth Edison Company, Zion Station Final Safety Analysis Report, Docket 50295-16 and 50304-16 (Chicago, IL, 1970)

B-10 M. G. Stevenson (editor) "Report of the Zion/Indian Point Study - Vol. II," NUREG/CR-1411, LA-8306-MS, Los Alamos National Laboratory, (Los Alamos, NM, April, 1980).

Distribution:
U. S. NRC Distribution Contractor (CDSI)
7300 Pearl Street
Bethesda, MD 20014
275 copies for R1

U. S. Nuclear Regulatory Commission (7)
Office of Nuclear Regulatory Research
Washington, DC 20555
Attn: R. M. Bernero
M. A. Cunningham
R. T. Curtis
C. N. Kelber
J. T. Larkins
D. F. Ross
L. S. Tong

U. S. Nuclear Regulatory Commission (5)
Office of Nuclear Regulatory Research
Washington, DC 20555
Attn: B. S. Burson
M. Silberberg
J. L. Telford
T. J. Walker
R. W. Wright

U. S. Nuclear Regulatory Commission (6)
Office of Nuclear Reactor Regulation
Washington, DC 20555
Attn: G. Quittschreiber

U. S. Nuclear Regulatory Commission (5)
Office of Nuclear Reactor Regulation
Washington, DC 20555
Attn: W. R. Butler
J. Rosenthal
Z. Rosztoczy
F. H. Rowsome
T. P. Speis

U. S. Department of Energy
Operational Safety Division
Albuquerque Operations Office
P.O. Box 5400
Albuquerque, NM 87185
Attn: J. R. Roeder, Director

Swedish State Power Board
El-Och Vaermeteknik
Sweden
Attn: Eric Ahlstroem

Berkeley Nuclear Laboratory (3)
Berkeley GL13 9PB
Gloucestershire
United Kingdom
Attn: J. E. Antill
S. J. Board
N. Buttery

Gesellschaft fur Reaktorsicherheit (GRS)
Postfach 101650
Glockengasse 2
5000 Koeln 1
Federal Republic of Germany
Attn: Dr. M. V. Banaschik

Battelle Institut E. V.
Am Roemerhof 35
6000 Frankfurt am Main 90
Federal Republic of Germany
Attn: Dr. Werner Baukal

UKAEA Safety & Reliability Directorate
Wigshaw Lane, Culcheth
Warrington WA3 4NE
Cheshire
United Kingdom
Attn: F. R. Allen
J. H. Gittus (6)
A. N. Hall
M. R. Hayns
K. McFarlane
R. S. Peckover

British Nuclear Fuels, Ltd.
Building 396
Springfield Works
Salwick, Preston
Lancs
United Kingdom
Attn: W. G. Cunliffe

AERE Harwell
Didcot
Oxfordshire OX11 ORA
United Kingdom
Attn: I. Cook (2)
J. R. Matthews, TPD

Kernforschungszentrum Karlsruhe
Postfach 3640
75 Karlsruhe
Federal Republic of Germany
Attn: Dr. S. Hagen (3)
Dr. J. P. Hosemann
Dr. M. Reimann

Simon Engineering Laboratory
University of Manchester
M13 9PL
United Kingdom
Attn: Prof. W. B. Hall (2)
S. Garnett

Kraftwerk Union
Hammerbacher strasse 12 & 14
Postfach 3220
D-8520 Erlangen 2
Federal Republic of Germany
Attn: Dr. K. Hassman (2)
Dr. M. Peehs

Gesellschaft fur Reaktorsickerheit (GRS mbH)
8046 Garching
Federal Republic of Germany
Attn: E. F. Hicken (2)
H. L. Jahn

Technische Universitaet Muenchen
D-8046 Garching
Federal Republic of Germany
Attn: Dr. H. Karwat

McGill University
315 Querbes
Outremont, Quebec
Canada H2V 3Wl
Attn: John H. S. Lee

National Nuclear Corp. Ltd.
Cambridge Road
Whetestone, Leicester, LE83LH
United Kingdom
Attn: F. P. O. Ashworth (2)
R. May

Director of Research, Science & Education
CEC
Rue De La Loi 200
1049 Brussels
Belgium
Attn: B. Tolley

Northwestern University
Chemical Engineering Department
Evanston, IL 60201
Attn: S. G. Bankoff

Brookhaven National Laboratory
Upton, NY 11973
Attn: R. A. Bari (3)
G. A. Greene
T. Pratt

UCLA
Nuclear Energy Laboratory
405 Hilgard Avenue
Los Angeles, CA 90024
Attn: I. Catton

Argonne National Laboratory
9700 South Cass Avenue
Argonne, IL 60439
Attn: R. P. Anderson (2)
Dae Cho

Sandia National Laboratories
Directorate 6400
P. O. Box 5800
Albuquerque, NM 87185
Attn: R. Cochrell (20)

University of Wisconsin
Nuclear Engineering Department
1500 Johnson Drive
Madison, WI 53706
Attn: M. L. Corradini

Los Alamos National Laboratory
P. O. Box 1663
Los Alamos, NM 87545
Attn: W. R. Bohl
M. G. Stevenson (2)

Battelle Columbus Laboratory
505 King Avenue
Columbus, OH 43201
Attn: P. Cybulskis (2)
R. Denning

Offshore Power Systems
8000 Arlington Expressway
Box 8000
Jacksonville, FL 32211
Attn: D. H. Walker

Electric Power Research Institute
3412 Hillview Avenue
Palo Alto, CA 94303
Attn: D. Squarer (4)
G. Thomas
R. Vogel
I. W. Wall

Fauske & Associates
627 Executive Drive
Willowbrook, IL 60521
Attn: R. Henry

General Electric Co.
175 Curtner Avenue
Mail Code 766
San Jose, CA 95125
Attn: R. Muraldiharan

NUS Corporation
4 Research Place
Rockville, MD 20850
Attn: G. W. Parry (2)
R. Sherry

Westinghouse Corporation
P. O. Box 355
Pittsburgh, PA 15230
Attn: N. Liparulo (3)
J. Olhoeft
V. Srinivas

TVA
400 Commerce Ave
W56178C-K
Knoxville, TN 37902
Attn: Dave Simpson

EG&G Idaho
Willow Creek Building, W-3
P. O. Box 1625
Idaho Falls, ID 83415
Attn: Richard Moore (2)
Server Sadik

Applied Sciences Association, Inc.
P. O. Box 2687
Palos Verdes Pen., CA 90274
Attn: D. Swanson

Purdue University
School of Nuclear Engineering
West Lafayette, IN 47907
Attn: T. G. Theofanous

UKAEA SRD
Wigshaw Lane
Culcheth, Warrington WA3 4NE
England, UK
Attn: A. J. Wickett (20)

UKAEA Culham Laboratories,
Abingdon, Oxon OX14 3DB,
England, UK
Attn: F. Briscoe (2)
B. D. Turland

School of Civil and Environmental Engineering
Cornell University
Hollister Hall
Ithaca, NY 14853
Attn: D. V. Swenson (10)

Technology for Energy Corporation,
One, Energy Center,
Pellissippi parklway,
Knoxville, TN 37922
Attn: A. M. Kolaczkowski, (2)
M. Fontana

University of Aston in Birmingham,
Department of Chemistry,
Gosta Green, Birmingham B4 7ET,
England, UK
Attn: A. T. Chamberlain (2)
F. M. Page

University of Loughborough
Department of Physics
Loughborough,
England, UK
Attn: J. Sturgess

H. M. Nuclear Installations Inspectorate,
Thames House North,
Millbank
London SW1
England, UK
Attn: R. D. Anthony (2)
S. A. Harbison

DECPU/SEFCA
C.E.N. Cadarache
BP No. 1.
13115 Saint-Paul- LEZ-Durance
France
Attn: Patrick Herter

Dr. Albert B. Reynolds
Dept. of Nuclear Engr. and Engr. Physics
Thornton Hall
University of Virginia
Charlottesville, VA 22904

H. Jacobs
KfK- INR,
Postfach 3640
D-7500 Karlsruhe 1
Federal Republic of Germany

Larry E. Hochreiter
Westinghouse Corporation
Nuclear Energy Systems
P.O. Box 350
Pittsburgh, PA 15230

Prof. E. Mayinger
Technische Universitaet Hannover
3000 Hannover 1
Federal Republic of Germany

M. Georges Berthoud
Laboratoire de Thermohydraulique des Metaux Liquides
Service des Transferts et Conversion d'Energie
Commissariat a l'Energie Atomique
Centre d' Etudes Nucleaires de Grenoble
B. P. N° 85 X - Centre de Tri
F-38041 Grenoble Cedex France

Dipl. Ing. Manfred Burger
Institut fur Kernenergetik und Energiesysteme
Universitate Stuttgart
Pfaffenwaldring 31
Postfack 801140
D-7000 Stuttgart 80 (Vaihingen)
Federal Republic of Germany

Dr. Ing. Leonardo Caldarola
Institut fur Reaktorentwicklung
Kernforschungszentrum Karlsruhe GmbH
Postfach 3640
D-7500 Karlsruhe 1
Federal Republic of Germany

Mr. Katsuro Takahashi
Research Associate
FBR Safety Laboratory
Oarai Engineering Center
P.N.C.
Oarai-Machi, Higashi
Ibaraki-Gun, Ibarake-ken
Japan

Ing. Giovanni Scarano
Il Direttore
Laboratorio Studi Dinamica e Sicurezza del Nocciolo
Divisione Ricerca e. Sviluppo
Dipartimento Reattori Veloci
Comitato Nazionale per l'Energia Nucleare
Centro di Studi Nucleari della Casaccia
S. P. Anguillarese km 1+3400
C. P. No. 2400
I-001000 Roma, Italy

Mr. Anthony J. Briggs/Mr. R. Potter (2)
UKAEA
Atomic Energy Establishment
Winfrith, Dorchester
Dorset DT2 8DH
United Kingdon

Dr. Ing. Heinz Kottowski
Head of Liquid Metal Section
Heat Transfer Division
Commission of the European Commmunities
Euratom-Joit Research Centre
Ispra Establishment
C. P. No. 1
I-21020 Ispra (Varese), Italy

David Yue
P.O. Box Y
Bldg. 9104-1
Oak Ridge, TN 37830

Bill Parkinson
SAI
5 Palo Alto Square, Suite 200
Palo Alto, CA 94304

Mr. Jacques Pelce
Department de Surete Nucleaire (DSN)
Institut de Protection et de Surete
Nucleaire (IPSN)
Commissariat a l'Energie Atomique
Centre d'Etudes Nucleaires de Fontenay-aux-Roses
Boite Postale 6
F-92260 Fontenay-aux-Roses, France

Dr. Hermann Rininsland
Head, Projekt Nukleare Sicherheit (PNS)
Kernforschungszentrum Karlsruhe G. M. B. H.
Postfach 3640
D-7500 Karlsruhe 1
Federal Republic of Germany

Mr. Carlo Zaffiro
Director, Safety Studies Division
Research & Development Sector
Direzione Centrale della Sicurezza
Nucleare e della Protezione Sanitaria (DISP)
ENEA
Viale Regina Margherita, 125
Casella Postale N. 2358
I-00100 Roma A.D.
Italy

Dr. Kazuo Sato
Deputy Director
Division of Nuclear Safety Evaluation
Japan Atomic Energy Research Institute
Tokai Establishment
Takai-mura
Naka-gun
Ibaraki-ken 319-11
Japan

Mr. Lars G. Hobgerg
Director, Office of Regulation and Research
Swedish Nuclear Power Inspectorate
Statens Karnkraftinspektion
P.O. Box 27106
S-102 52 Stockholm
Sweden

Mr. Andrew C. Mullunzi
Director, LWR Safety Research and Development
Office of Converter Reactor Deployment
Mail Stop B-107
U. S. Department of Energy
Washington, D. C. 20545

Mrs. Paola Fasoli-Stella
Manager, Reactor Safety Programme
Commission of the European Communities
Euratom Joint Research Centre
Ispra Establishment
Casella Postale 1
I-21027 Ispra
Italy

Dr. Jacques Royen
Nuclear Safety Division
OECD Nuclear Energy Agency
38 Boulevard Suchet
F-75016 Paris,
France

Sandia National Laboratories Distribution:

1524 W. N. Sullivan
6400 A. W. Snyder
6410 J. W. Hickman
6411 V. L. Behr
6411 A. S. Benjamin
6411 A. L. Camp
6411 F. E. Haskin
6412 S. W. Hatch
6415 J. M. Griesmeyer
6420 J. B. Rivard
6420 J. V. Walker
6421 K. Maramatsu
6421 T. R. Schmidt
6422 D. A. Powers
6423 P. S. Pickard
6425 W. J. Camp
6425 W. Frid
6425 R. J. Lipinski
6425 K. Schoenefeld
6425 S. D. Unwin
6425 M. F. Young
6427 M. Berman (20)
6427 M. S. Krein
6427 B. W. Marshall Jr.
6427 L. S. Nelson
6427 O. Seebold
6427 M. P. Sherman
6427 C. C. Wong
6440 D. A. Dahlgren
6442 W. A. von Riesemann
6444 L. D. Buxton
6444 S. L. Thompson
6449 K. D. Bergeron
6449 D. C. Williams
7223 R. G. Easterling
8424 M. A. Pound
3141 C. M. Ostrander (5)
3151 W. L. Garner

NRC FORM 335 (2.84) NRCM 1102, 3201, 3202

U.S. NUCLEAR REGULATORY COMMISSION

BIBLIOGRAPHIC DATA SHEET

SEE INSTRUCTIONS ON THE REVERSE

1. REPORT NUMBER (Assigned by TIDC, add Vol. No., if any)
NUREG/CR-3369
SAND83-1438

2. TITLE AND SUBTITLE
AN UNCERTAINTY STUDY OF PWR STEAM EXPLOSIONS

3. LEAVE BLANK

4. DATE REPORT COMPLETED
MONTH | YEAR

5. AUTHOR(S)
M. Berman, D. V. Swenson, and A. J. Wickett

6. DATE REPORT ISSUED
MONTH: May | YEAR: 1984

7. PERFORMING ORGANIZATION NAME AND MAILING ADDRESS (Include Zip Code)
Sandia National Laboratories
Albuquerque, NM 87185

8. PROJECT/TASK/WORK UNIT NUMBER

9. FIN OR GRANT NUMBER
A1030

10. SPONSORING ORGANIZATION NAME AND MAILING ADDRESS (Include Zip Code)
Division of Accident Evaluation
Office of Nuclear Regulatory Research
U.S. Nuclear Regulatory Commission
Washington, DC 20555

11a. TYPE OF REPORT
Technical

b. PERIOD COVERED (Inclusive dates)

12. SUPPLEMENTARY NOTES

13. ABSTRACT (200 words or less)

Some previous assessments of the probability of containment failure caused by in-vessel steam explosions in a PWR have recognized large uncertainties and assigned broad ranges to the probability, while others have concluded that the probability is small or zero. In this report we study the uncertainty in the probability of containment failure by combining the uncertainties in the component physical processes using a Monte Carlo method. We conclude that, despite substantial research, the combined uncertainty is still large. Some areas are identified in which improvements in our understanding may lead to large reductions in the overall uncertainty.

14. DOCUMENT ANALYSIS - a. KEYWORDS/DESCRIPTORS
steam explosions
vapor explosion
PWR
uncertainty analysis
failure modes

b. IDENTIFIERS/OPEN-ENDED TERMS

15. AVAILABILITY STATEMENT
Unlimited

16. SECURITY CLASSIFICATION
(This page) Unclassified
(This report) Unclassified

17. NUMBER OF PAGES
89

18. PRICE

☆U.S. GOVERNMENT PRINTING OFFICE: 1984-0-776-027/4311

Org.	Bldg.	Name	Rec'd by	Org.	Bldg.	Name	Rec'd by

120555078877 1 1AN1R1
US NRC
ADM-DIV OF TIDC
POLICY & PUB MGT BR-PDR NUREG
W-501
WASHINGTON DC 20555

Sandia National Laboratories